DYNAMIC RESPONSE OF BLUFF BODIES TO WAVE FORCES

Qureshi G. Ahmad

A MAJOR TECHNICAL REPORT

in the

Faculty of Engineering

Presented in partial fulfilment of the requirements for
the Degree of Master of Engineering at
Sir George Williams University
Montreal, Canada

April 1974

ABSTRACT

Qureshi G. Ahmad

DYNAMIC RESPONSE OF BLUFF BODIES TO WAVE FORCES

Equipment was designed to determine the wave profile and wave forces on simple bluff bodies. The preliminary experiments were conducted on a circular pile of 6 inches. The depth of water was varied up to 45.5 inches and the height of the sinusoidal waves were limited to 9 inches. The wave force and wave profile records indicate that the instrumentation and equipment developed did function satisfactorily. Both the drag force and lift force could be measured. For the latter, the tests should be limited to a frequency range of not more than 1.15 cycles per second, since the natural frequency of the force gage-cylinder system was of the order of 2.3 cycles per second.

The test data presented should be considered as a preliminary result. Since the force gauge and wave gauge have linear response, the tests with random waves can also be handled by the set-up developed.

ACKNOWLEDGEMENTS

ACKNOWLEDGEMENTS

The author wishes to express his very sincere thanks to Professor A.S. Ramamurthy of the Department of Civil Engineering, at Sir George Williams University; and Professor A. Leclerc, Ecôle Polytechnique, for suggesting this study.

The permission to use the excellent channel facilities, and assistance of trained laboratory staff of L'Ecôle Polytechnique is gratefully acknowledged.

Thanks are also given to Sir George Williams University for the fabrication of the test pile and force gauges by Mr. Ted Mani.

This research was supported in part, under Grant No. A-7608 by the National Research Council.

TABLE OF CONTENTS

TABLE OF CONTENTS

LLST OF FIGURES

LIST OF FIGURES

LIST OF TABLES

LIST OF TABLES

LIST OF SYMBOLS

LIST OF SYMBOLS

A	projected area per unit length of pile, ft^2
cps	cycles per second
C_e	experimentally observed wave celerity - ft/sec.
C_L	coefficient of lift, dimensionless
$\bar{C}_{L_{max}}$	average max. coeff. of lift, dimensionless
C_T	theoretical wave celerity - ft/sec.
C_D	coefficient of drag, dimensionless
C_M	coefficient of inertia, dimensionless
h	water depth, ft.
D	pile diameter, ft.
$F(t)_o$	horizontal component of the force on the pile, lb.
f	frequency, cycle/second (Hertz)
f_e	frequency of eddy shedding, cycles/sec.
f_N	natural frequency of system, cycles/sec.
F_i	inertial force, lb.
F_d	drag force, lb.
F_L	lift force, lb.
H	wave amplitude
L_e	experimental value of wave length, ft.
L	wave length
R_e	Reynolds' Number dimensionless
T	wave period, sec.
t	time, sec.

u	horizontal comp. of water particle veloc., ft/sec.
u_{max}	maximum horizontal vel. of water particle, ft/sec.
$u_{max}T/D$	Keulegan-Carpenter number, dimensionless
$u_{max}D/\nu$	Reynolds number, dimensionless
v	vertical component - water particle velocity ft/sec.
V	water velocity in uniform steady flow, ft/sec.
$\frac{\partial v}{\partial t} = \dot{v}$	vertical component - water particle acceleration ft/sec^2
V_1	velocity component normal to the axis of test body
z	distance from bottom of flume to bottom of pile inches
θ	2π x/L, phase angle
$\frac{\partial u}{\partial t} = \dot{u}$	horizontal component of water particle acceleration, ft/sec^2
ρ	mass density
ν	kinematic viscosity, ft^2/sec.

CHAPTER 1

INTRODUCTION

CHAPTER 1

INTRODUCTION

1.1 INTRODUCTION

This project was directed towards the development of instrumentation and experimental equipment to collect and interpret wave force data on a vertical and yawed circular ocean pile model. Increasing recognition has been given recently to the importance of marine resources in terms of oil and food. This has stimulated the construction of a large number of off-shore structures. Although there is a considerable amount of data related to the mechanics of wave action on bluff structural forms used in assembling off-shore structures, a great deal of scatter is associated with the results relating to the force coefficients published by several [2,24] investigators. This indicates that there is a good deal of scope to unify the existing data.

Much of the discrepancy in the functional relationships claimed by past investigators is attributed [13,26] to the excessive reliance on wave theory to obtain the kinematics of flow near the body (based on surface observation of the wave) and the inadequacy of the testing procedures.

1.2 GENERAL SCOPE OF STUDIES

As a part of a short development program, the following tasks were set out for the general scope of studies.

It was decided to develop a wave force model which would allow the investigator to obtain the following data.

1) To determine the distribution of pressure along the cylindrical pile model.

2) To find the effect of inclination of the test pile on the nature of wave forces.

3) To collect new information on the wave characteristic and wave force measurements, using more accurate measuring systems.

4) To check the total force response data with the force bounds established by local pressure measurements.

5) To cover some range of waves not covered in the literature.

6) To develop a force gauge capable of measuring lateral forces; and testing expected response characteristics considering vortex shedding frequency and wave periods.

7) To develop an accurate wave gauge which would have a linear response over the range of selected waves.

8) To study the resonance phenomenon due to lateral vibrational forces.

CHAPTER 2

THEORETICAL CONSIDERATIONS

CHAPTER 2

THEORETICAL CONSIDERATIONS

2.1 OSCILLATORY WAVE MOTION

At present there are several wave theories, which can be selected for design wave representation. All these theories are applied based on general guide-lines of depth conditions.

There is an intuitive belief that the additional effort required to use higher order wave theories should be rewarded by more accurate results. Most of the theories are quite difficult to apply. The differences in particular design parameters predicted by several theories are not determined readily. Studies [7], were made to determine relative validities of water wave theories. As a result of these studies experimental verification was recommended.

One experimental study [24] as to the validity of linear (Airy) wave theory was conducted and found velocity and acceleration profiles "differ considerably" from theory. However, the presented plots in this study seem to show considerable degree of agreement in relation to wave kinematics predicted by the linear theory. Others [5,16,17,26] too, have applied the Airy (linear) theory to define wave parameters with success.

In this project, the actual wave celerity was determined by recording the wave history by two wave gauges. This value was used to determine the wave length for a known period wave. The calculated wave length was used as a first approximation of wave length to get the theoretical value of wave celerity using Airy theory as follows:

C_e denotes experimentally determined wave celerity.

T denotes wave time period.

$$L_e = C_e \cdot T \qquad (2.1)$$

L_e is experimental value of wave length.

From the Airy theory

$$C_T = \left[\frac{gL}{2\pi} \tanh \frac{2\pi h}{L}\right]^{\frac{1}{2}} \qquad (2.2a)$$

C_T denotes the theoretical wave celerity.

h equals the depth of still water in the channel.

Substitution of $L \approx L_e$ gives

$$C_T = \left[\frac{gL_e}{2\pi} \tanh \frac{2\pi h}{L_e}\right]^{\frac{1}{2}} \qquad (2.2b)$$

Physical observations were made and the wave record was generally sinusoidal (Fig. 2.1). Physical observations of the approximate wave length checked with the theoretical value of L obtained from equations 2.1 and 2.2a. Tables 2 and 3 gives a comparison between the measured wave length and the theoretical value of the same.

The range of dimensionless water depths encountered in the tests was

$$0.481 < h/L < 0.097$$

This range precludes the approximations for the deep water or shallow water waves. As such, the complete wave equation (2.2a) was used.

$$\therefore \quad u = \frac{\pi H}{T} \frac{\cosh \frac{2\pi (y+h)}{L}}{\sinh \frac{2\pi h}{L}} \cos\theta \qquad (2.3)$$

$$v = \frac{\pi H}{T} \frac{\sinh \frac{2\pi (y+h)}{L}}{\sinh \frac{2\pi h}{L}} \sin\theta \qquad (2.4)$$

$\theta = 2\pi X/L$ is phase angle, where u and v are horizontal and vertical partial velocities, respectively.

The differentiation with regard to t gives the accelerations

$$\frac{\partial u}{\partial t} = \frac{2\pi^2 H}{T^2} \frac{\cosh [2\pi(y+h)/L]}{\sinh(2\pi h/L)} \sin\theta \qquad (2.5)$$

$$\frac{\partial v}{\partial t} = \frac{2\pi^2 H}{T^2} \frac{\sinh [2\pi(y+h)/L]}{\sinh(2\pi h/L)} \cos\theta \qquad (2.6)$$

2.2 OSCILLATORY WAVE FORCES
LONGITUDINAL FORCES

The Reynold's numbers range based on maximum particle velocities varied from 10^4 to 10^5 (Tables 2 and 3). The drag coefficient C_D is constant for steady flow in the above Reynolds number range (Fig. 2.2).

One should not overlook the fact that the value of the instantaneous Reynolds number, based on particle velocity reaches the value of zero twice during a cycle for wave motion.

The forces produced on submerged structures by oscillatory waves are properly classified by Morrison [19]. According to him, the drag force resulting from the orbital velocity; and the inertial force resulting from the orbital acceleration can be expressed as

$$F_d = C_d A \rho \frac{U^2}{2} \qquad (2.7)$$

The inertial force is expressed as

$$F_i = C_m \rho V_o \frac{\partial u}{\partial t} \qquad (2.8)$$

where

A	denotes projected area of test body
F_d	denotes drag force
C_d	denotes drag coefficient
ρ	is the mass density of water
u	denotes component of the velocity in the direction of the force
F_i	denotes inertial force
C_m	denotes coefficient of inertial resistance
V_o	is displaced volume
$\frac{\partial u}{\partial t}$	denotes component of acceleration in the direction of force for undisturbed flow

Because of the nature of the velocity variation, the horizontal drag force varies from a maximum downstream value under the crest of a wave ($x/L = 0$) to a maximum upstream value under a trough ($x/L = 0.50$) (Fig.2.3).

The variation of the horizontal acceleration (Eq. 2.6) is such that the horizontal inertial force varies from a maximum downstream value at ($x/L = \frac{1}{4}$) to a maximum upstream value at ($x/L = \frac{3}{4}$) as illustrated in Figure 2.3.

The total force is the sum of the two forces given by Eqs. (2.7) and (2.8)

$$F = C_d A \rho \frac{U^2}{2} + C_m \rho V_o \frac{\partial u}{\partial t} \qquad (2.9)$$

Because the two forces are 90^o out of phase, the maximum combined down stream force may occur at any value of x from x/L = 1 to x/L = $\frac{1}{4}$, depending on the relative magnitude of the components. Methods of applying Eq. (2.9) to determine the magnitude and location of the maximum force on cylindrical piles have been presented by Morrison et al [20].

2.3 LATERAL FORCES

Lateral or lift forces are not negligible. Wiegal et al [25] in their study of wave forces at an exposed location near Davenport, California, reported large lateral vibrations of their test pile until the pile was restrained at the lower end. This and the failure of the Texas Tower No. 4 off the coast of New Jersey on January 15th, 1961, due to lateral vibrations are but two examples of wave induced lateral forces.

When the frequency of lateral vibration approaches the system frequency of the structure, resonance occurs. This may lead to disastrous consequences. Overlooking the possibility of such vibrations may lead to serious cracking of

the structural members under fatigue.

It is well established that lift forces are due to alternate eddy shedding as the waves pass the pile.

A commonly used equation for lift forces [8] is

$$F_L = \tfrac{1}{2} C_L \rho u^2 A \qquad (2.10)$$

F_L denotes lateral or lift force

C_L denotes lift coefficient

u and ρ are previously defined

The above equation gives rise to difficulties as the time history of the forces does not necessarily vanish when u goes through zero. Thus, very large values can be obtained for the coefficient of lift. This difficulty can be largely overcome by defining the relationship of Eq. (2.10) only for the maximum values of the force.

$$\therefore \quad F_{L\,max} = \tfrac{1}{2} \cdot C_{L\,max} \cdot \rho \cdot U^2_{max} \cdot A \qquad (2.11)$$

2.4 OBLIQUE FORCES

In addition to vertical piling members, a structure will be composed of cross-bracing. This bracing may be orientated horizontally or obliquely through the fields of velocity and acceleration.

Due to the fact that all of the wave force investigations on vertical piling have calculated C_D using the horizontal component of velocity, Eq. (2.7) was used in this study. Unfortunately, the situation is not the same for oblique cylinders (Fig. 2.4). For an oblique cylinder set in water waves, the resultant velocity is clearly larger than the component normal to the cylinder axis. Taking account of this Eq. (2.7) can be rewritten as

$$F_d = C_d A \rho \frac{(u^2 + v^2 + w^2)}{2} \frac{V_1}{|V_1|} \qquad (2.12)$$

where V_1 is the velocity component normal to the axis of test body. The term $V_1/|V_1|$ establishes the force direction as that of the normal velocity component. The quantities u,v,w are the velocity components in the coordinate axis direction.

For practical purposes velocity component w could be considered negligible and equation (2.12) can be written as

$$F_d = C_d A \rho \frac{(u^2 + v^2)}{2} \frac{V_1}{|V_1|} \qquad (2.13)$$

u and v are determined by using equations (2.3) and (2.4).

The effect of yaw upon inertia force component could in the same manner be determined. The rewriting of

Eq. (2.8) as

$$F_i = C_m \rho V_o \sqrt{\dot{u}^2 + \dot{v}^2} \qquad (2.14)$$

The yaw angle is the angle between the normal to the test body axis and the resultant velocity. It should be noted that in all cases, plane wave motion is assumed, and a coordinate system is chosen (one axis in the direction of wave propagation) for which there are only two components of velocity and acceleration. It is assumed that the axis of the test body is located at x = 0 and that the diameter is much smaller than the wave length.

CHAPTER 3

REVIEW OF PRIOR WORK

CHAPTER 3

REVIEW OF PRIOR WORK

3.1 LONGITUDINAL FORCES

Wiegal, Beebe and Moon [24] measured the forces exerted by ocean waves on circular cylindrical piles at an exposed location near Davenport, California, in water depths up to a maximum of fifty feet. They made measurements of forces resulting from wave heights up to twenty feet. Morrison's equation was used to evaluate C_D and C_m.

Both C_D and C_m were found to have no well defined relationship with Reynold's number in the test range of Reynold's number from 3×10^4 to 9×10^5.

Keulegan and Carpenter [18] investigated the drag and inertia coefficients of cylinders in a simple sinusoidal current generated at the midsection of a rectangular basin by surging of standing waves.

Their experiments showed that the average values of C_m and C_D over a wave cycle could be correlated with the parameter $U_{max} \times T/D$ (see Fig. 3.1(a),(b)), where U_{max} is the maximum horizontal partical velocity over a wave cycle. This study was able to cover a wide range of values of $U_{max} \times T/D$ between 2.7 and 120.0. $U_{max} \times T/D$ equaling 15 was found to be a critical condition yielding the lowest,

value of C_m and the largest value of C_D. The range of Reynold's number $U_{max} \times D/\nu$ was between 4200 and 29,300.

Iverson and Balent [14] developed a resistance equation for objects moving in accelerated unidirectional motion. MacCarmy and Fuchs [21] presented a theory of wave forces acting on a circular cylindrical pile for the case when the pile diameter is considerably large compared with the wave length. In a prototype, this theory applies to the case of caissons. Their theory considers only the inertia forces of primary and secondary waves while the drag component becomes negligible. When $h/L \to 0$, the MacCarmy and Fuchs caisson theory is reduced to a simple form identical with the Morrison formula (Eq. 2.9) ($C_d = 0$ and $C_m = 2.0$).

In 1957, Bretschneider [3] calculated Morrison's C_D and C_m for a 16 in. pile in 40 ft of water from his recorded maximum range of total forces. The average height of all waves analyzed by him was about 4.5 ft with maximum 13.3 ft and minimum of 1.2 ft. The wave periods were between 4.0 to 9.8 seconds. C_D was found to bear a relationship with Reynold's number $U_r h/\nu$ somewhat similar to that for steady state conditions between 2×10^6 and 6×10^6. Here, U_r is the root mean square partical velocity. A relationship between C_m and the water partical acceleration was also indicated in his study.

Harleman and Shapiro [11] performed a series of experiments for the case of $h/L = 0.2$ and $H/L = 0.03$. They proposed a procedure which incorporates the MacCarmy and Fuchs theory for the inertia component and utilizes a drag component which is similar in form to Morrison's, but makes use of the steady state drag coefficients for cylinders. Stokes' second order wave theory was used in this case. A surprising degree of accuracy was reached in predicting the total forces of their experiments ($U_{max}\, h/\nu = 4.77 \times 10^3 \sim 8.06 \times 10^4$, $H/D = 1.66 \sim 12.5$). Jen Yvan [15,16] found that forces due to periodic waves in relatively deep water ($h/L = 0.175$) and low steepness ($H/L = 0.02$) were essentially inertial. Morrison's C_m values were found to have an overall average value of 2.04 which is very close to the theoretical estimates [19]. The values of C_D reported in [15,16] displayed a very large scatter. It is observed that C_D values tend to be large for waves of small amplitude.

3.2 LATERAL FORCES (LIFT)

The problem of lift forces on a cylinder when it is subject to uniform and accelerated unidirectional flow has been treated in several papers. However, insufficient information is available on the topic of lift forces on piles subject to waves.

Humphreys [12] studied the forces associated with sub-critical flow around a circular cylinder in a wind tunnel. He studied the oscillating forces due to the down-stream vortex street for Reynold's numbers ranging from 4×10^4 to 6×10^5, which covered the critical range of Reynold's numbers of 2×10^5 to 4×10^5. The steady drag, the oscillating lift at the eddy shedding frequency, f_e and the small oscillating drag at frequency $2 f_e$ were measured.

Fung [9] carried out laboratory tests with a 125" diameter pile in a wind tunnel. He measured fluctuating lift and drag forces in an air flow at large Reynold's numbers (supercritical). He found that the most important feature of the forces induced on a circular cylinder by vortex shedding for super-critical Reynold's numbers was their randomness. The peak values of the RMS coeffient of lift were below 0.4 for all cases.

Bishop and Hassan [2] measured fluctuating lift and drag forces for a stationary cylinder in a water channel for Reynold's numbers from 3.6×10^3 to 1.1×10^4. The frequencies of the vortices in the wake were obtained indirectly by noting the frequency of the lift fluctuating force, as shown on the records. The coefficient of lift was found to decrease as the Reynold's number decreased within the range tested. (Fig. 3.2). Gerrard [10] deter-

mined from measurements in a wind tunnel, the lift and drag on circular cylinders, and the fluctuating pressure on the cylinder surface in the Reynold's number range from 4×10^3 to 10^5. The magnitude of RMS lift coefficient was found to have a maximum value of about 0.8 at a Reynold's number of 7×10^4, decreasing to 0.01 at a Reynold's number of 4×10^3.

Macovsky [22] has presented measurements of the maximum alternating lift force coefficient for a body immersed in a moving stream for Reynold's numbers ranging from 10^4 to 10^5. He found that the values of the lift forces were comparable in magnitude to the longitudinal force (drag force).

Jen, using the work of Wiegel [25] concluded that the wave height had to be at least three times as great as the pile diameter for eddies to have time to develop. He carried out his experiments with a 6" diameter pile, which was large compared with wave dimensions. The maximum value of H/D that Jen could reach was about 1.2. However, he found that even with this ratio, some effect of eddies was detected in the force records.

Chang [6] formulated two theoretical approaches to investigate the traverse forces on circular cylinders due to eddy shedding in waves. One approach assumed a quasi-

steady vortex shedding frequency. Experiment with regular waves, however, showed that this theory could not be applied. The other approach involved the use of a constant vortex shedding frequency. He drew the conclusion that the frequency of the transverse force was twice the wave frequency for all cases. Chang's plots of coefficient of lift as a function of Keulegan-Carpenter number and Reynold's number are presented in Figs. 3.3(a) and (b).

Bidde [4] concluded that the Keulegan-Carpenter number appears to be a useful parameter to predict the ratio of lift to longitudinal forces. According to him the eddies start forming when the Keulegan-Carpenter number reaches 3. Further, the maximum of lift to longitudinal forces occurs when the Keulegan-Carpenter number becomes 15. He also concluded that the Reynold's number failed to correlate with the ratio of lift to longitudinal forces for the piles tested.

3.3 OBLIQUE FORCES

To-date, no detailed study of the forces on oblique cylinders such as the ones used as bracings in off-shore structures, is reported. Dean and Harleman [13] have suggested an approach to tackle this problem. McCormick [23] has given an empirical approach to solve this problem.

CHAPTER 4

EXPERIMENTAL EQUIPMENT AND INSTRUMENTATION

CHAPTER 4

EXPERIMENTAL EQUIPMENT AND INSTRUMENTATION

4.1 WAVE GENERATOR AND TOWING TANK

The tests of this study were performed in a towing tank 185 ft long. It was 8 ft wide and 6 ft deep. (Figs.4.1(a-c)). The towing tank was equipped with a piston type wave generator at one end, and an inclined rubberized plastic fiber (Fig. 4.1(c)) beach for absorbing the wave energy at the other end. Beach assembly at the end was such that the inclination of the beach could be varied. Along one side of the tank about 70' from the wave generator was the observation section. The pile assembly (Fig. 4.2) was mounted rigidly at the mid-point of a bridge which has its own motorized assembly and for this study was locked in at a point about the middle of the tank length. The pile extended down to the bottom of the tank with a 3/16 inch clearance (z). The assembly was made rigid enough to assure that the deflection of the pile throughout the series of tests was small and behaved as a rigid pile.

The wave generator was provided with a servo- mechanism Fig. 4.1(a).This servo-mechanism could either,be operated by a magnetic tape or by external voltage sources.(Fig.4.1(f)).For this study, the mechanism was programmed for the desired single wave period response, and these waves were repeatedly generat-

ed.

The bridge (Fig. 4.1(e)) was mounted on rails and had a motorized set-up for towing the pile. Motorized wheels of the bridge provided a range of towing velocities. For this study, the bridge was fixed at about mid-length of the tank and no towing tests were performed.

4.2 THE PILE ASSEMBLY

A 6-inch outer diameter aluminium test pile was designed and built for this study; Figures 4.2 shows details of its design. The pile was 4'-6" long. Sets of 36 peripheral holes were provided at different locations along the length of the pile to measure the local pressure distribution at different depths of submersion. These holes were connected to plastic tubing which could be fitted to the tap holes at the top of the pile. For this study, the tubings were closed and only the total forces were measured.

4.3 INSTRUMENTATION

4.3.1 Force Gauge

For force measurements, a force gauge was developed, using a linear voltage differential transducer. The gauge was fixed to the collar of the pile. The frame to which the gauge was fixed was capable of being easily rotated to

measure the lateral forces subsequent to the measurement of the drag forces, without having to take the test section out of the water (Fig. 4.1(e)).

Because the design of the force gauge required consideration of the resonant frequency of the assembly, which behaves like a spring-mass system, the stainless steel force gauge frame was provided with stiffener attachments. This arrangement not only allows the natural frequency of the system to be high enough but also allows it to be stiff enough in order to reduce the deflections of the test pile during the experiments.

The force gauge was checked for the range of linear response with the stiffeners and without the stiffeners, as shown in Fig. 4.3. This range varied from 0 to 90 lbs and from 0 to 30 lbs, respectively. The natural frequency of the system in the water was found to be 2.3 cycles per second; which became the governing limit of wave frequency, Fig. 4.4. The corresponding depth was 3.79 ft.

The calibration of the force gauge was performed with the test section submerged, using a pulley system, as shown in Fig. 4.5. The adjustable pin was used to provide a true zero location of the transducer for zero load position.

The load was applied at the end of the cord and corresponding gauge outputs were recorded on a strip chart

recorder (Model Brush-Mark 220 Recorder). In the beginning of this study, calibrations were made before each run, which later were reduced to twice per day or as required. Throughout this study, the gauge response was found to be constant. The high stability and rugged construction of the gauge did not present any problem throughout this study.

4.3.2 Wave Gauges

Two capacitance-type gauges were used to measure the profile of the incident wave train.

The construction of these gauges was based on the Purdue University supplied circuits. The basic circuits provided were developed and adapted for this project. The instrument consists of solid state circuitry and printed circuit boards (Fig.4.1(g)).

The probe functions as a capacitor with the water functioning as a negative plate. The insulation of the positive conductor functions as the dielectric, with the wire functioning as the positive plate. The changing levels of water, alter the physical size of both the positive and negative plates. This change is then detected by the capacitance gauge (Fig.4.1(e)).

The capacitance gauge consists of a Wien-bridge oscillator, which is an operational amplifier running in a

state of saturation. The output of the oscillator is fed through zero suppression and filter. The signal becomes a carrier and is fed to the primary of the low impedance transformer. The probe signal is applied to the secondary of this transformer.

The resulting signal is fed through the A.C. Amplifier for a gain of approximately 5x. The amplified signal is then demodulated, which is now a varying D.C. voltage riding at a level determined by the current sources of the filter and suppression board.

The resulting D.C. voltage is amplified by D.C. amplifier and fed through a low pass filter to provide the output of the capacitance gauge. Because of interdependency of the internal circuits, it is necessary to "rock in" the D.C. level and A.C. gain controls.

The D.C. output carries a noise level of less than 0.005 millivolts. This gauge utilizes a common chassis and signal ground. With the circuits of this gauge and the probe (signal source), both grounded, it is apparent that some amount of ground-loop current will be generated due to the difference in potential at the two points of grounding.

The water surface probe consisted of a single copper ground wire and a double length of insulated wire. A streamlining foil was added to the basic assembly to reduce the

flow disturbances due to flow separation behind the probe support. (Fig. 4.1(e). The dialectric and inner conductor of RG 174/4 coaxial cable was found to be the most satisfactory positive conductor wire. To avoid problems due to surface tension, ordinary water repellent silicon compound was used and found to be satisfactory.

The calibration of gauges was made by increasing a known depth of immersion of the probe and recording the response of the gauge.

These gauges were found to be linear in the entire range of wave heights (12") used. Fig. 4.6 indicates the gauge response.

In the beginning, these gauges were calibrated at the beginning of each run. But later, they were calibrated after every 4 runs.

One gauge was located parallel to the test pile and the other at about 10 ft up-stream of the test section.

Wave trains were recorded and the wave celerity was determined.

To determine the capacitance gauge response lag differences (if any), between the two wave gauges, the gauges were placed parallel and wave trains were recorded. The resulting response records are shown in Fig. 4.7.

4.4 EXPERIMENTAL PARAMETER SELECTION

4.4.1 Wave Parameters

The dimension of wave tank and location of observation windows required that the water depth for all experiments vary between 50" to 28". Therefore, 4 depths of 45", 40", 35" and 30" were chosen.

The wave generator could generate waves having 4 seconds to 1/3 second period. The waves of period less than 1 second were not used for this study. The chosen periods were 4,3,2 and 1 seconds to avoid the range of Reynolds numbers belonging to the super-critical regions.

The maximum amplitude for the above chosen wave periods, which could be controlled independently by the servo-mechanism, was 12 inches. However, depending upon the depth of the water, 8 inch amplitudes were generally considered as the limit.

4.4.2 System Interaction

A block diagram of the system interaction is given below:

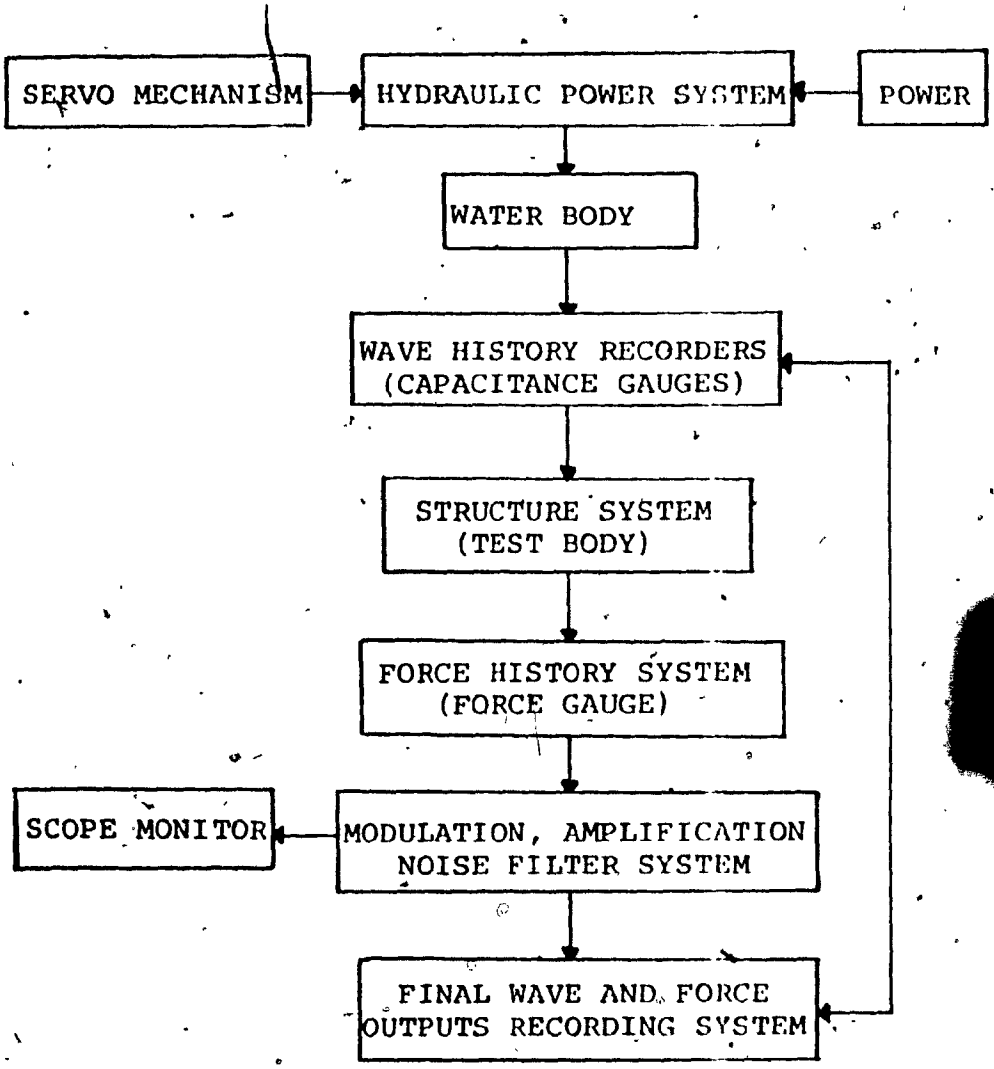

Figure 4.1 (g) shows the instrumentation set-up.

In general, the total system functioned well. Despite very sensitive set-ups and complicated circuiting, the initial time to debug the whole system was relatively short. All the gauges and instrumentation functioned with a high degree of stability.

CHAPTER 5

RESULTS AND DISCUSSIONS

CHAPTER 5

RESULTS AND DISCUSSIONS

5.1 RESULTS OF PRELIMINARY TESTS

The range of variables for the present study is shown in Figure 5.1.

5.2 LONGITUDINAL FORCES

Longitudinal forces were measured for the pile set at both vertical position and non-zero yaw position. The yaw was limited to 14° measured from vertical.

The drag coefficient is plotted against Reynold's number R. For plotted data from the present experiments there appears to be some correlation between C_D and Reynold's number (Fig. 5.2).

The pile was swung from the vertical (zero yaw) position to the 6.5°, 10° and 14° inclinations and forces due to the waves were measured. From this total force data, the drag coefficient C_D was obtained and plotted against the corresponding Keulegan Number. The drag coefficient C_D for zero yaw case is also plotted (Fig. 5.3).

From this figure, it appears that yaw introduces regular reduction of the drag coefficient. This reduction is nearly constant between Keulegan Numbers of 3 to 9.

The maximum values of drag coefficient C_D, were associated with zero yaw (vertical pile).

5.3 LATERAL FORCES

During the same tests, the lateral forces for the pile were also recorded. The lift coefficient C_L calculated from this data is plotted against the Keulegan Number and the Reynold's Number (Fig. 5.4).

Both the Keulegan Number and the Reynold's Number show considerable scatter. The numerical value of C_L drops from a maximum of 0.8 to 0.5 between the Keulegan Number of 1.0 to 5.0. The same drop of C_L corresponds to the Reynold's Number range of 10^4 to 2×10^4 (Fig. 5.5).

Photographic observations (Fig. 5.6 (a) and (b)) with regard to eddy formation lead to the following conclusions:

1) Keulegan Number < 2, no separation - amplitude of motion less than pile diameter.

2) Keulegan Number 2-3 - some separation, at least one eddy is shed.

3) Keulegan Number 3-4 - more than 2 eddies are shed within the half-cycle.

4) Keulegan Number slightly in excess of 4 - wake becoming turbulent. Additional eddies are shed where swept back.

5) Keulegan Number - very large values - extremely TURBULENT.

5.4 REPORTED RESULTS

Only the results of a few tests are reported. The reduced data for all the tests conducted are reported elsewhere [27].

CHAPTER 6

CONCLUSIONS

CHAPTER 6

CONCLUSIONS

The equipment for measurement of wave forces on cylindrical piles was developed to provide wave profile and wave force records.

1) Up to a range of 9 inches the wave heights can be registered and the gauge output was linear and noise-free.

2) The use of two wave gauges provided a means to determine the wave length, L; independently. These values of 'L' checked well with the expected values of 'L' from the Airy Theory.

3) The force gauge was extremely sensitive and had a natural frequency 'F_n' of 2.31 cycles per second, considered adequate to measure oscillating forces up to the vortex shedding frequency of about half the natural frequency (= 1.15 cps). The gauge was linear up to 35 lbs.

4) With minor modifications, one can measure forces on piles which were set at specific yaw angles to the oncoming wave train.

5) A few preliminary tests were made to check the type of wave force and wave profile records that could be obtained. The tests included both lift and drag force measurements.

CHAPTER 7

NEEDS FOR FURTHER STUDY

CHAPTER 7

NEEDS FOR FURTHER STUDY

It is necessary to investigate in detail the dependence of C_D and C_m on both the Reynold's number and the Keulegen-Carpenter Number. To obtain a better understanding of these functional relationships, the experimental work should be directed towards direct measurements of particle velocities and accelerations.

Besides studying the total average forces, studies should be directed towards measuring the local pressures on the surface of the test body.

In earlier studies [17,26] large values of C_D were reported, as in the present study, especially when small amplitude waves were considered. Some studies should be directed to find the cause of this error or confirm the present findings.

For waves of relatively large wave lengths a simplified solution for yawed test body response was adopted in the present study.

The study should be extended to cover smaller wave lengths and the results should be checked on the basis of a plausible theory.

Modifications to the design of the force gage should be made to measure both the longitudinal and transverse forces, simultaneously.

The integration of pressure at different depths yields the force per unit length of the pile. A detailed study of this force distribution is necessary since the force components are expected to possess a span-wise distribution.

BIBLIOGRAPHY

BIBLIOGRAPHY

[1] Borgman, Leon Emry, "Ocean Wave Simulation for Engineering Design". Proc. of Conf. on Civ. Engg. in the Oceans, ASCE Conf. San Francisco, Calif. Sept. 6-8, 1967.

[2] Bishop, R.E.D. and Hassan, A.Y., "The Lift and Drag Forces on a Circular Cylinder Oscillating in a Flowing Fluid", Proc. Roy. Soc. Lond., Series A, Vo. 277, 1964; pp.51-75.

[3] Bretschneider, C.L., "An Evaluation of Inertial Coefficients in Wave Force Experiments", Texas A & M Tech. Rep. 55-3, Sept. 1955.

[4] Bidde, D.D., "Wave Forces on a Circular Pile Due to Eddy Shedding". Univ. Calif. Berkeley.Dissertation Submitted in partial satisfaction of the requirements for the degree of Doctor of Philosophy, 1970.

[5] Bidde, Devidas, "Laboratory Study of Lift Forces on Circular Piles", J. Waterways and Harbors Div.,Proc. ASCE, WW4, November 1971.

[6] Chang, K.S., "Transverse Forces on Cylinders due to Vortex Shedding in Waves". M.S. Thesis submitted to the Mass. Inst. of Tech. January 1964.

[7] Dean, Robert G., "Relative Validity of Water Wave Theories", ASCE Conf. Proc. Civ. Engg. in the Oceans, Calif. Sept. 7-8, 1967.

[8] Daily, J.W., and Harleman Fluid Dynamics Addison - Wesley Publishing Company, Inc., Addison-Wesley (Canada) Limited, Don Mills, Ontario, 1966.

[9] Fung, Y.C., "Fluctuating Life and Drag Acting on a Cylinder in a Flow at Supercritical Reynolds Numbers". J. Aerospace Sciences, Vol. 27, Nov. 1960, pp.801-814.

[10] Gerrard, J.H., "An Experimental Investigation of the Oscillating Life and Drag of a Circular Cylinder Shedding Turbulent Vortices". J. Fl. Mechs. Vol. 11, p.2, Sept. 1961, pp.51-75.

[11] Harleman, D.R.F., and Shapiro, W.C., "Experiment and Analytical Studies of Wave Forces on Offshore Structures", Part 1, Results for Vertical Cylinders, May 1955, Mass. Inst. Tech. Hydrodynamic Laboratory Techn. Rep. No. 19.

[12] Humphreys, J.S., "On a Circular Cylinder in a Steady Wind at Transition Reynolds Numbers". J.Fluid Mechanics, Vol. 9, No. 4, 1960, pp.603-612.

[13] Ippen, A.T. ed. Estuary and Coastline Hydrodynamics, McGraw-Hill Book Co., Inc., N.Y. 1966.

[14] Iversen, H.W., and Balent, R., "A Correlating Modulus for Fluid Resistance in Accelerated Motion", J.Appl. Physics, 22,3, March 1951.

[15] Jen, Yuan, Dissertation - Doctor of Philosophy in Engineering in the Graduate Division of the Univ. of Calif., Berkeley, "Wave Forces on a Circular Cylindrical Pile".

[16] Jen, Yvan, "Laboratory Study of Inertia Forces on a Pile", J. Waterways and Harbours Div. Proc. ASCE, WW1, February 1968.

[17] Johnson, E.R., "Horizontal Forces due to Waves Acting on Large Vertical Cylinders in Deep Water", J. Basic Engg. 72-WA/Oct.3, ASME Publ.

[18] Keulegan, G.H., and Carpenter, L.H., "Forces on Cylinders and Plates in an Oscillating Fluid", J. Res. Nat. Bur. Standards, 60, 5, 423-440, May 1958.

[19] Lamb, Sir Horace, "Hydrodynamics", 6th ed. New York. Dover. Publications Inc. 1945.

[20] Morrison, J.R., O'Brien, M.P., Johnson, J.W., and Shaaf, S.A., "The Force Exerted by Surface Waves on Piles", Petroleum Trans. 189, TP 2846, pp.149-154, 1950.

[21] MacCamy, R.C., and Fuchs, R.A., "Wave Forces on Piles: A Diffraction Theory", U.S. Army Corps of Engineers, Beach Erosion Board, Technical Memo No. 69, Dec. 1954.

[22] Macovsky, M.C., "Vortex-Induced Vibration Studies". David Taylor Model Basin, Rep. No. 1190, July 1958.

[23] McCormick, M.E., "Ocean Engineering Wave Mechanics", John Wiley, 1973.

[24] Pratte, B.D., Funke, E.R., Mogridge, G.R., and Jamieson, W.W., "Wave Forces on a Model Pile", Can. Hydr.Conf.Univ. Alberta, Edmonton, May 10-11, 1973.

[25] Wiegel, R.L., "Waves and Their Effects on Pile Supported Structures", Proc. Symp. Res. on Wave Action, Vol. 1, pp.1-43, Delft Hydraulics Laboratory, July 1969.

[26] Wiegel, R.L., Beebe, K.E., and Moon, James (1957), "Ocean Wave Forces on Circular Cylindrical Piles", J. Hyd. Div. ASCE, 83, HY2, Paper 1199, 1937.

[27] Ramamurthy, A.S., and Qureshi, G.A., Report No. E.F.M.-2-CE74-1, Sir George Williams University, Civ. Engg. April, 1974.

APPENDIX A

FIGURES

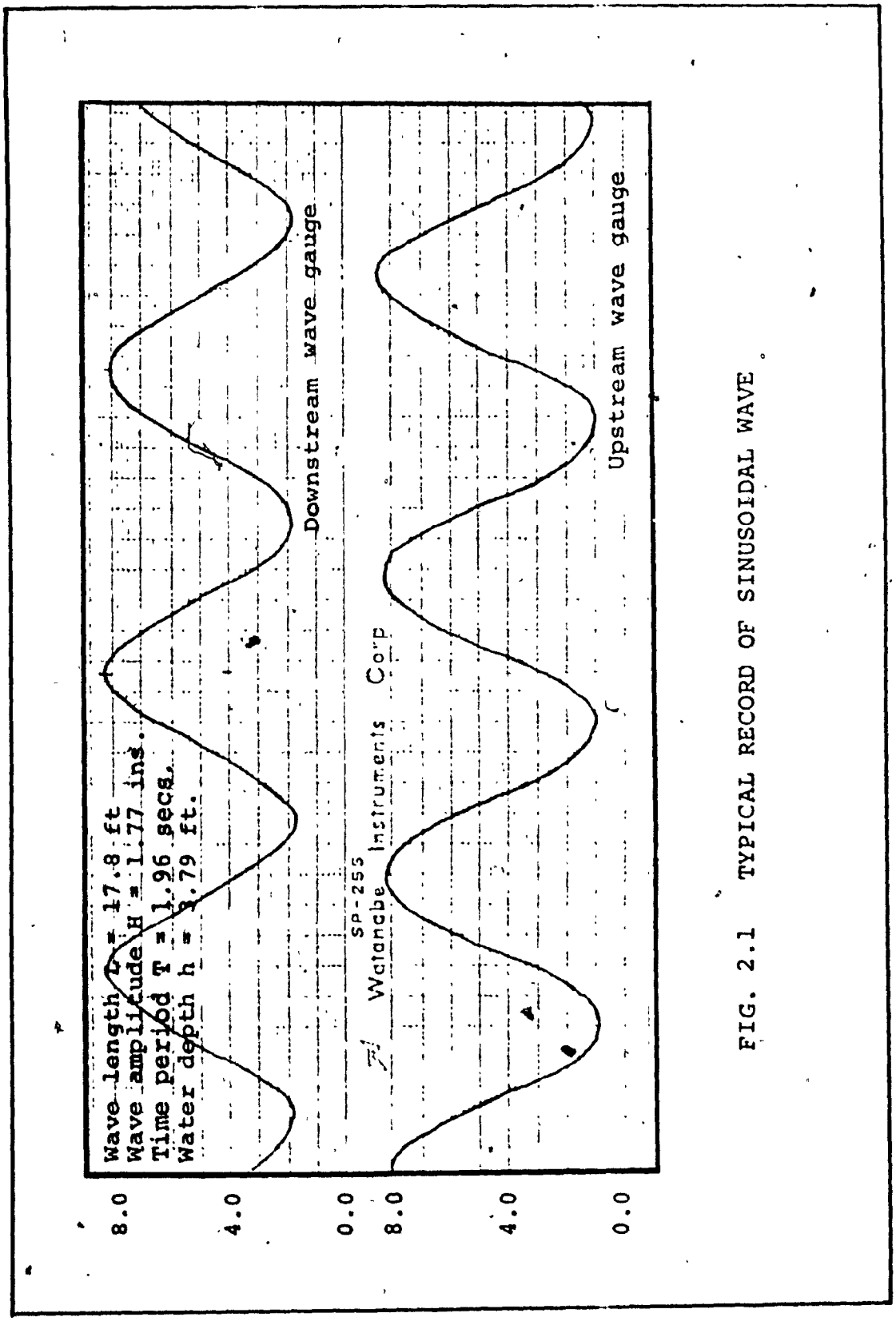

FIG. 2.1 TYPICAL RECORD OF SINUSOIDAL WAVE

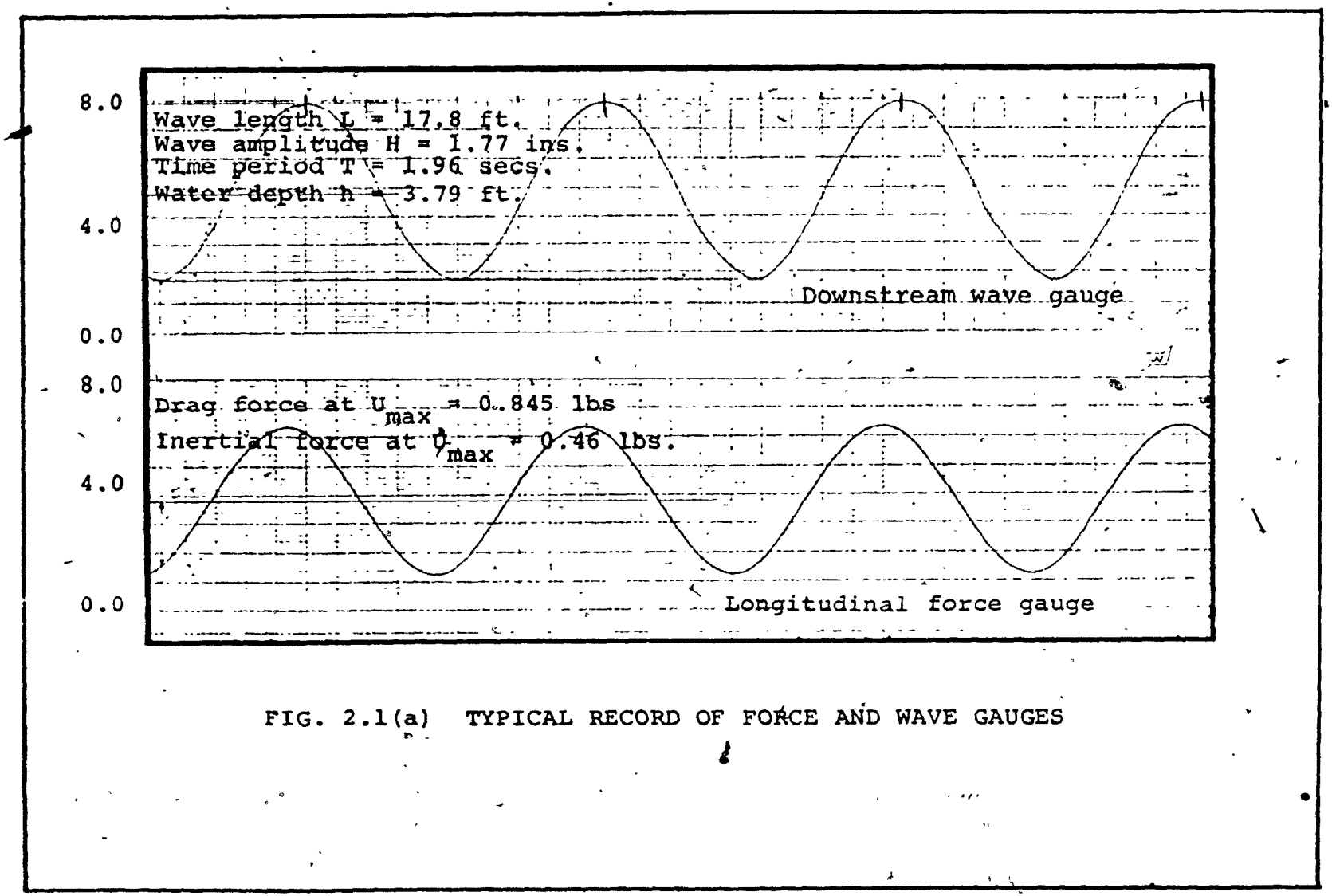

FIG. 2.1(a) TYPICAL RECORD OF FORCE AND WAVE GAUGES

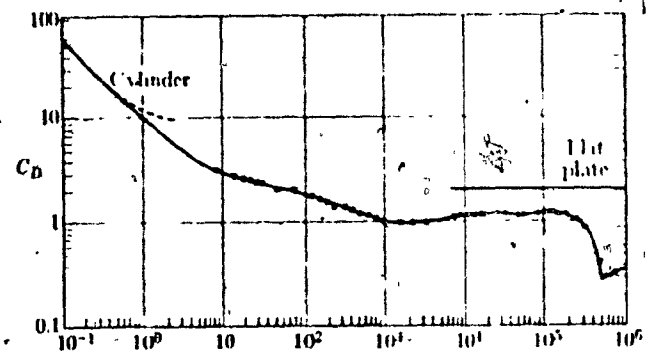

FIG. 2.2 DRAG COEFFICIENTS FOR CIRCULAR CYLINDER AND FLAT PLATES NORMAL TO FLOW (2-DIMENSIONAL)-STEADY FLOW [8]

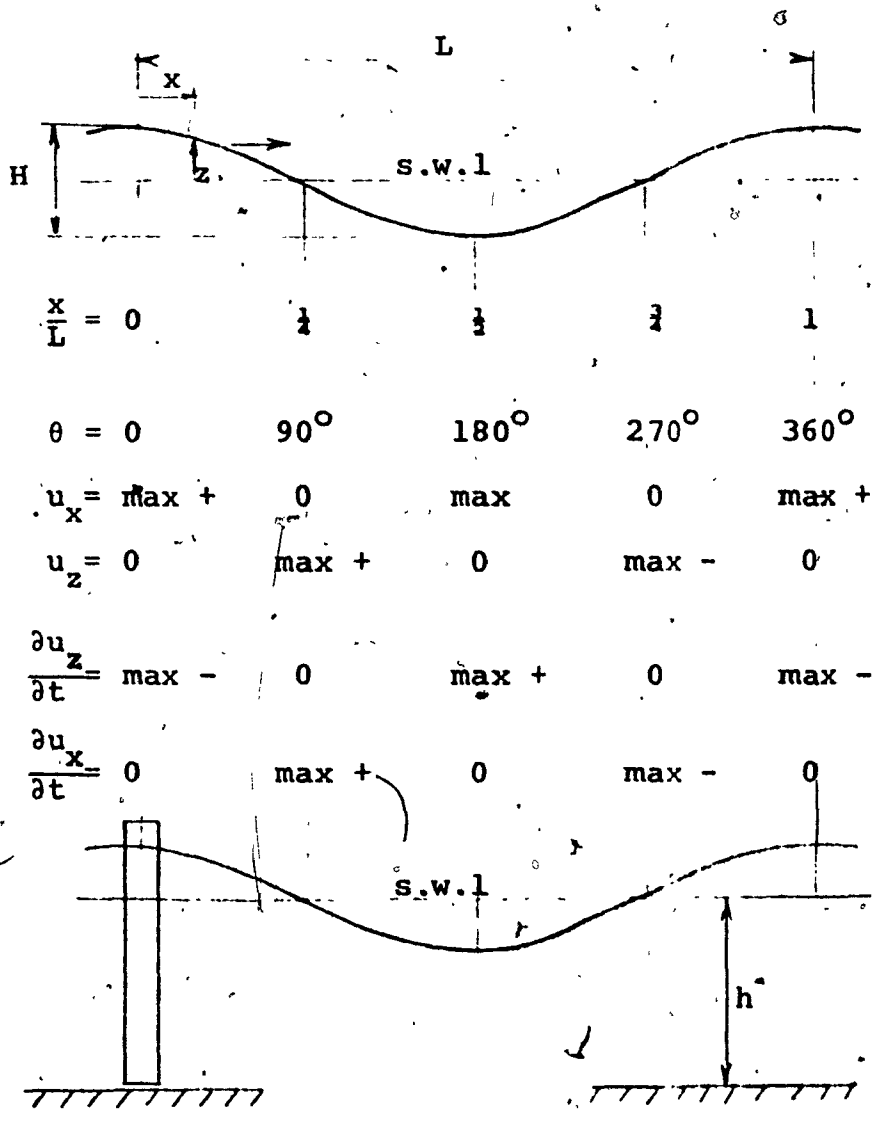

FIG. 2.3 OSCILLATORY WAVES

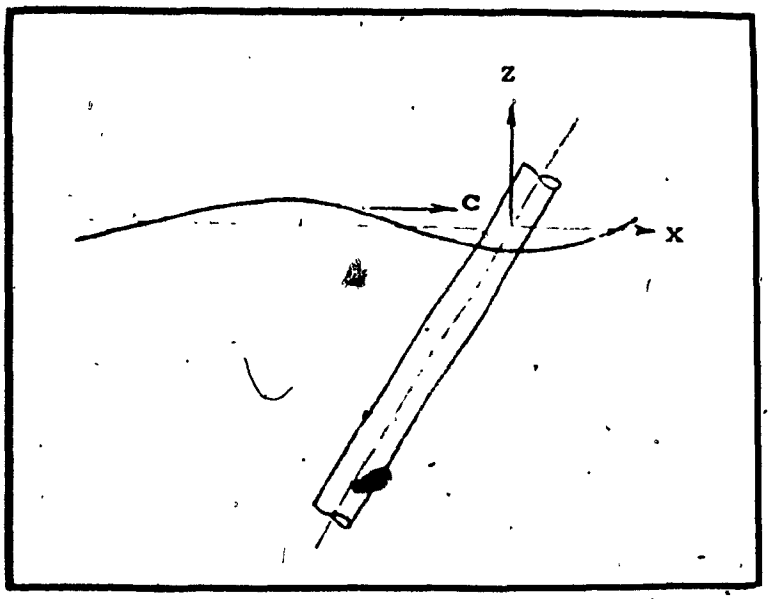

FIG. 2.4 AN INCLINED CIRCULAR PILE IN WAVES

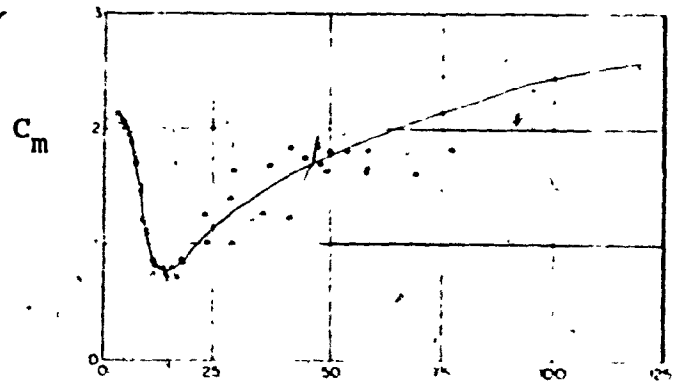

Keulegan Number

FIG. 3.1(a) VARIATION OF INERTIA COEFFICIENT OF CYLINDERS

Diameter(inches): 3 2.5 2 1.75 1.5 1.25 1 0.75 0.5
Corresponding symbol: ○ △ □ ◇ ● ▲ ■ ◆ ✦

(AFTER KEULEGAN-CARPENTER) [18]

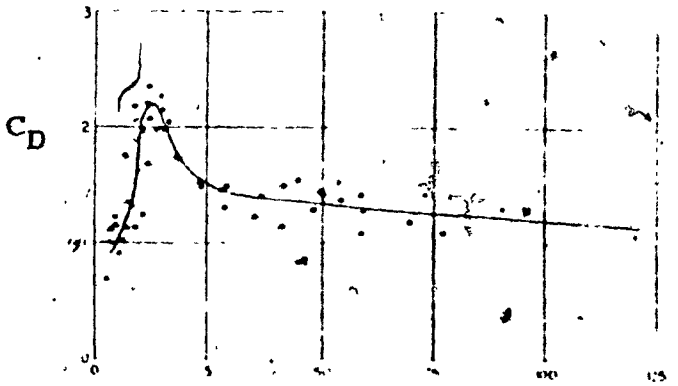

Keulegan Number

FIG. 3.1(b) VARIATION OF DRAG COEFFICIENT OF CYLINDERS

Diameter(inches): 3 2.5 2 1.75 1.5 1.25 1 0.75 0.5
Corresponding Symbol: ○ △ □ ◇ ● ▲ ■ ◆ ✦

(AFTER KEULEGAN-CARPENTER) [18]

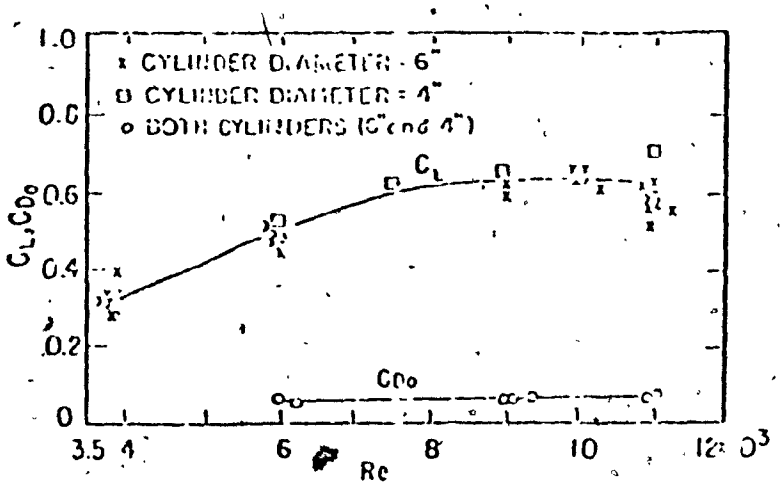

FIG. 3.2 COEFFICIENT OF LIFT AND OF FLUCTUATING DRAG VS. REYNOLD'S NUMBER

(AFTER BISHOP AND HASSAN) [2]

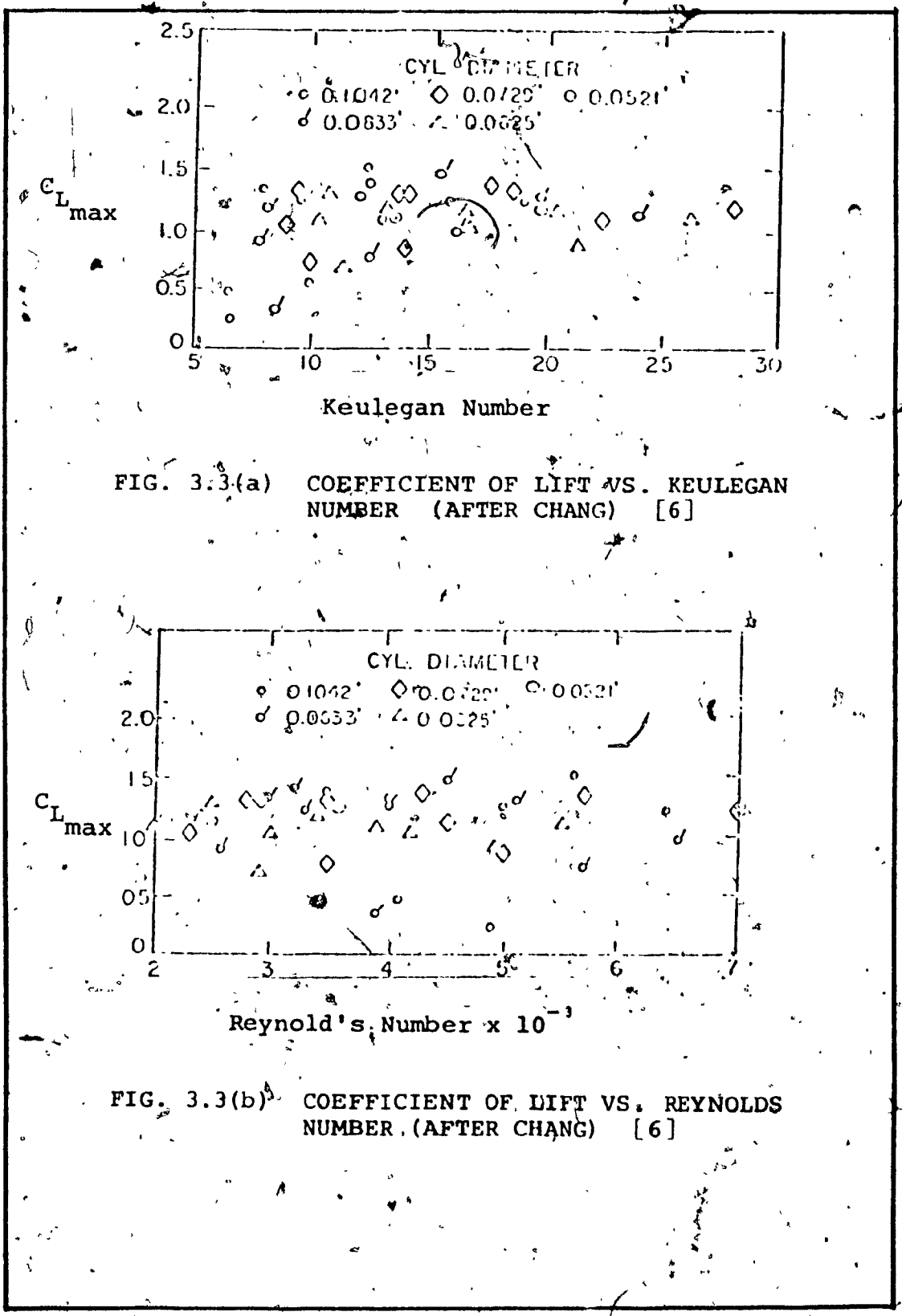

FIG. 3.3(a) COEFFICIENT OF LIFT VS. KEULEGAN NUMBER (AFTER CHANG) [6]

FIG. 3.3(b) COEFFICIENT OF LIFT VS. REYNOLDS NUMBER (AFTER CHANG) [6]

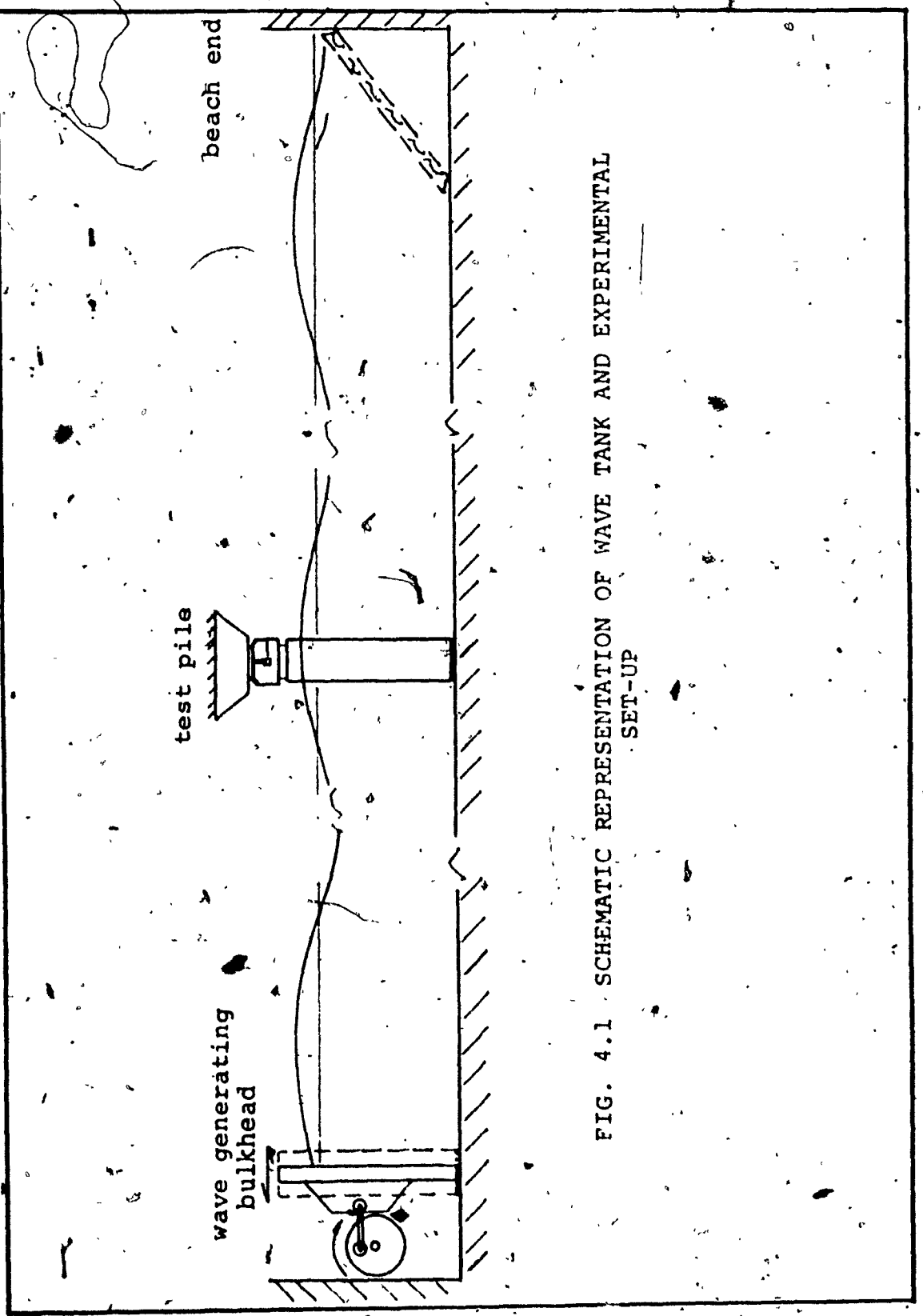

FIG. 4.1 SCHEMATIC REPRESENTATION OF WAVE TANK AND EXPERIMENTAL SET-UP

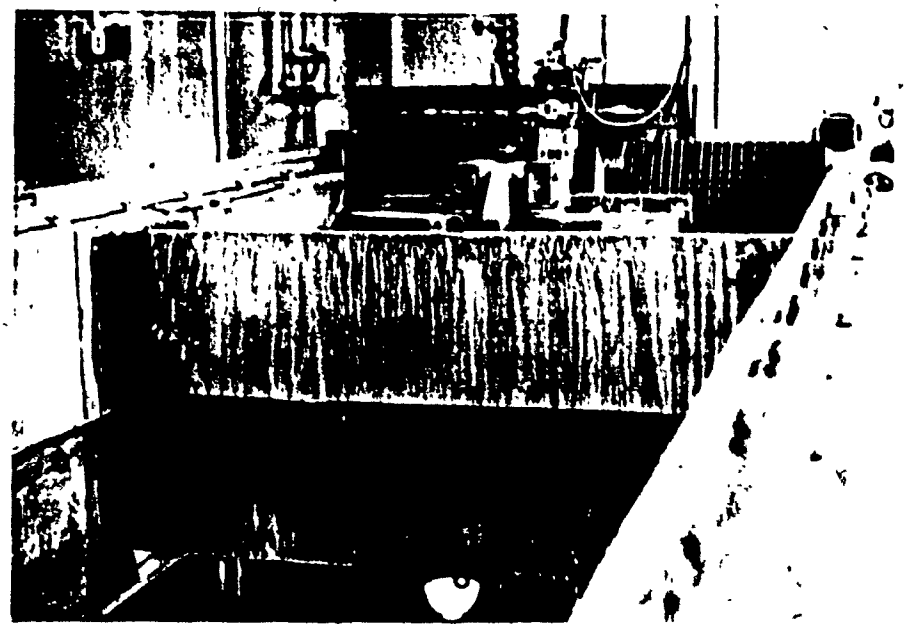

FIG. 4.1(a) WAVE GENERATING BULKHEAD

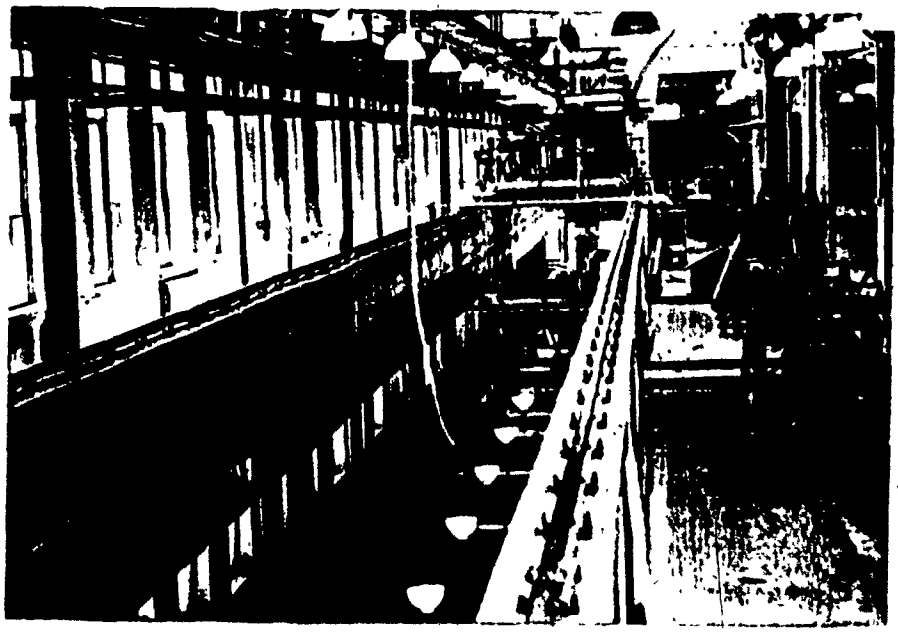

FIG. 4.1(b) VIEW OF WAVE TANK FROM WAVE GENERATING END

FIG. 4.1(c) BEACH END OF TANK

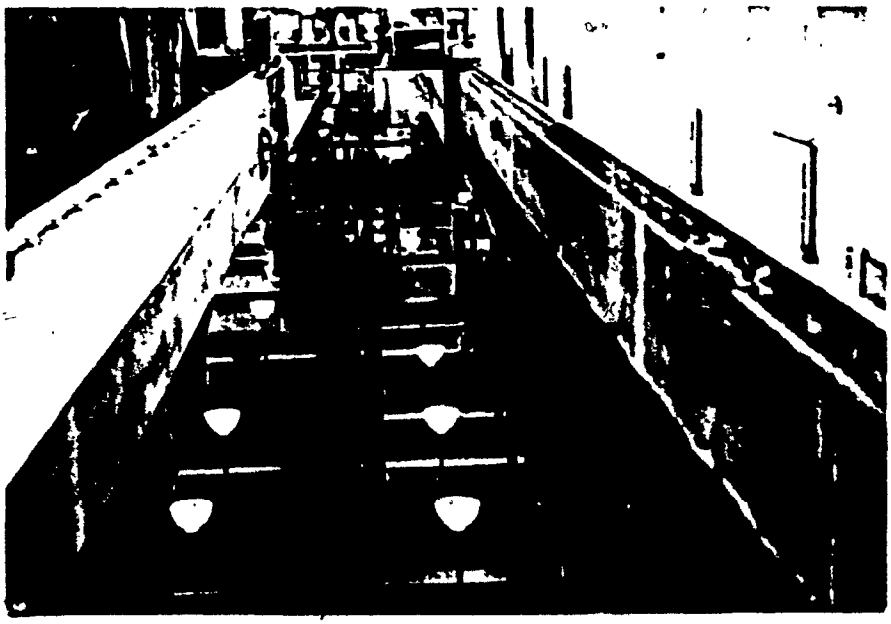

FIG. 4.1(d) VIEW OF TANK FROM BEACH END

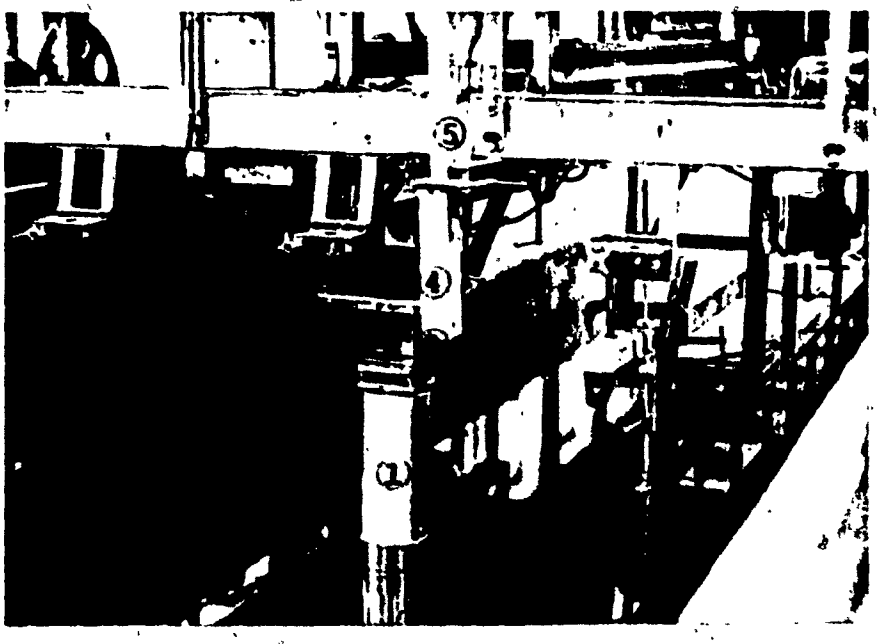

FIG. 4.1 (e) TEST SET-UP

(1) Test Pile
(2) Force Gauge
(3) Water Profile Probe
(4) Mounting for Yaw Testing
(5) Bridge and Its Motorized System
(6) Stream Lining Foil

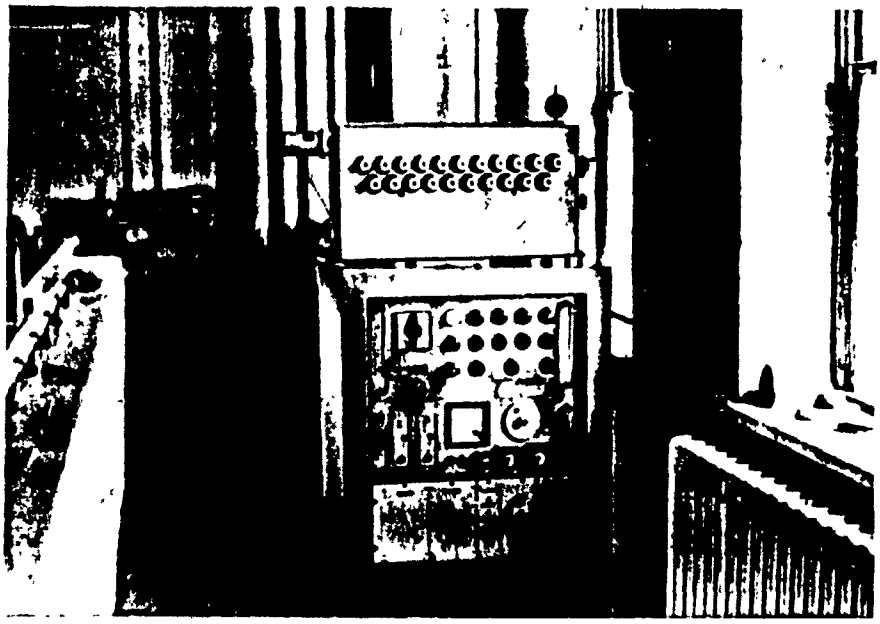

FIG. 4.1 (f) WAVE POWER AND SERVO SYSTEM

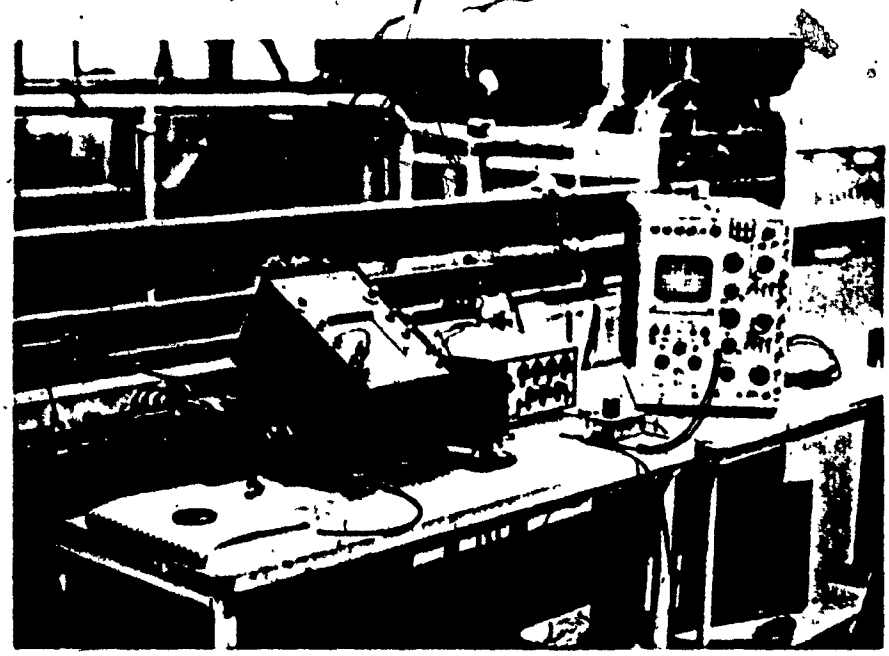

FIG. 4.1 (g) INSTRUMENTATION SET-UP

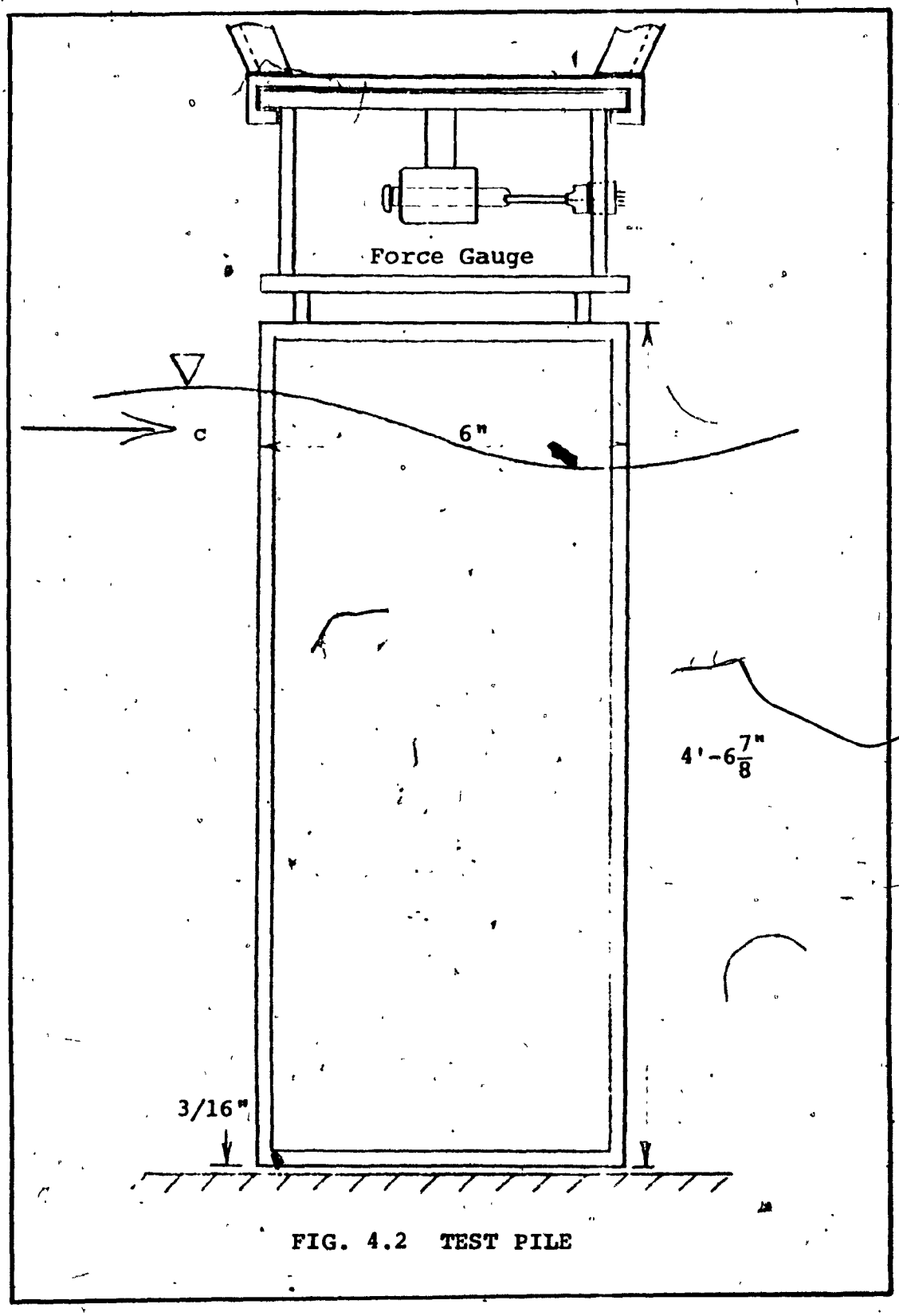

FIG. 4.2 TEST PILE

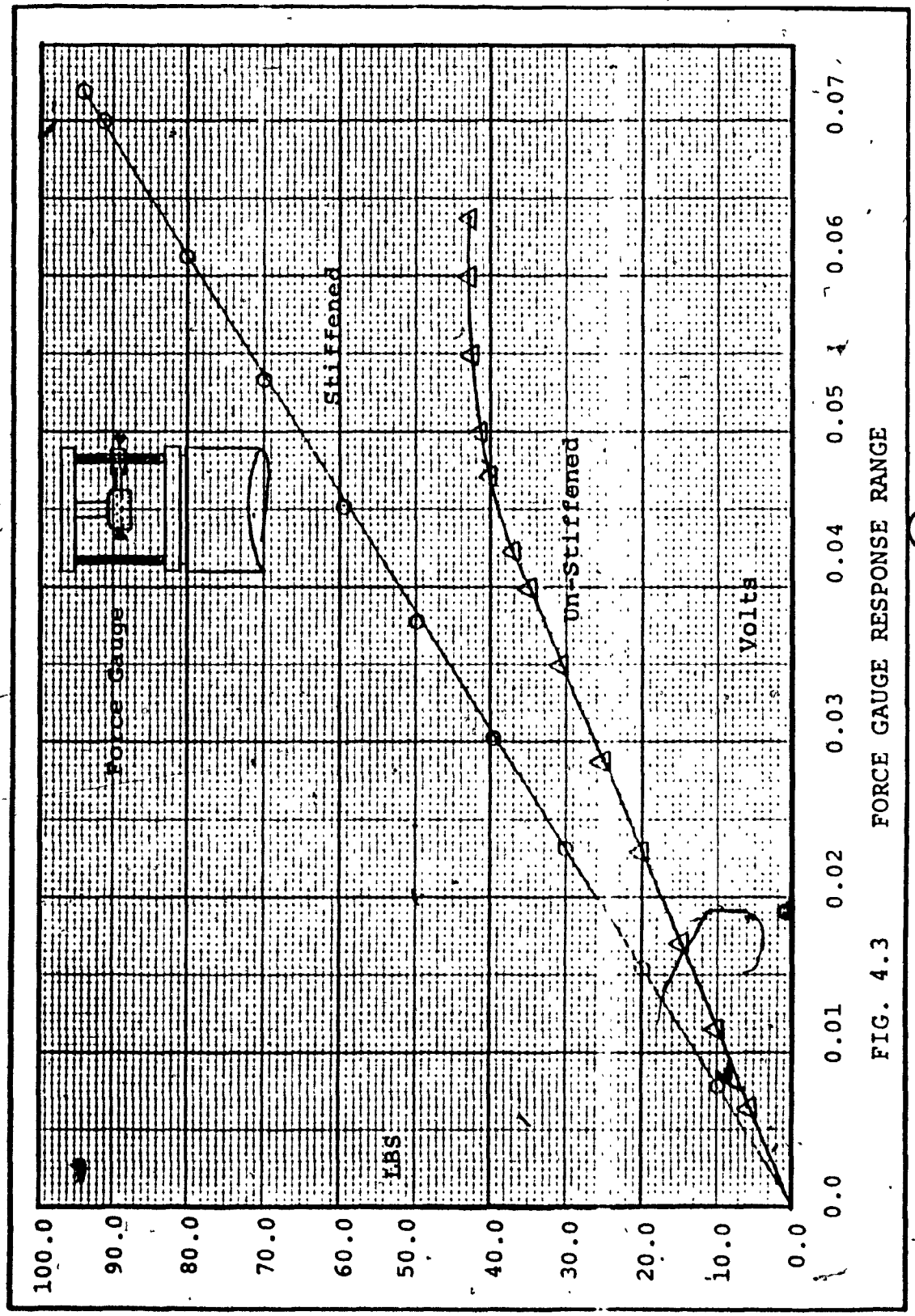

FIG. 4.3 FORCE GAUGE RESPONSE RANGE

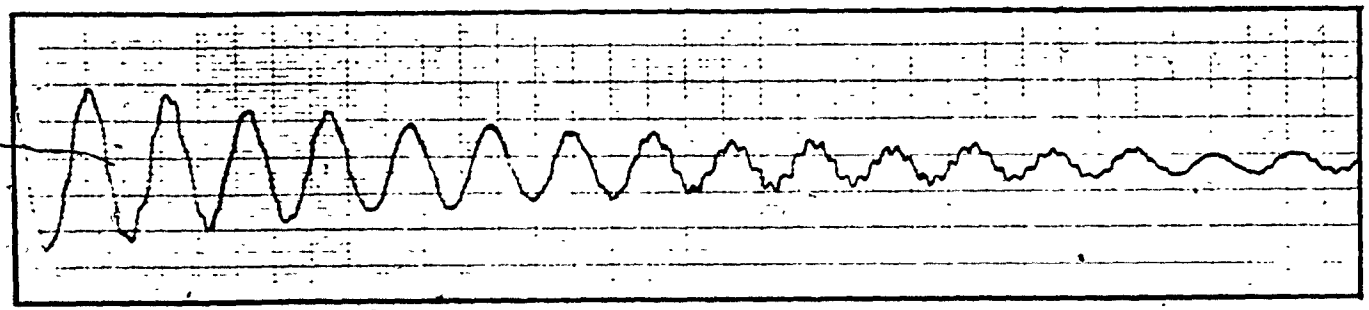

Chart speed 25 mm/sec.

6 Cycles in 65 mm

$\therefore \frac{6 \times 25}{65} = 2.31$ cps $= F_n$ of system

FIG.4.4 NATURAL FREQUENCY OF SYSTEM

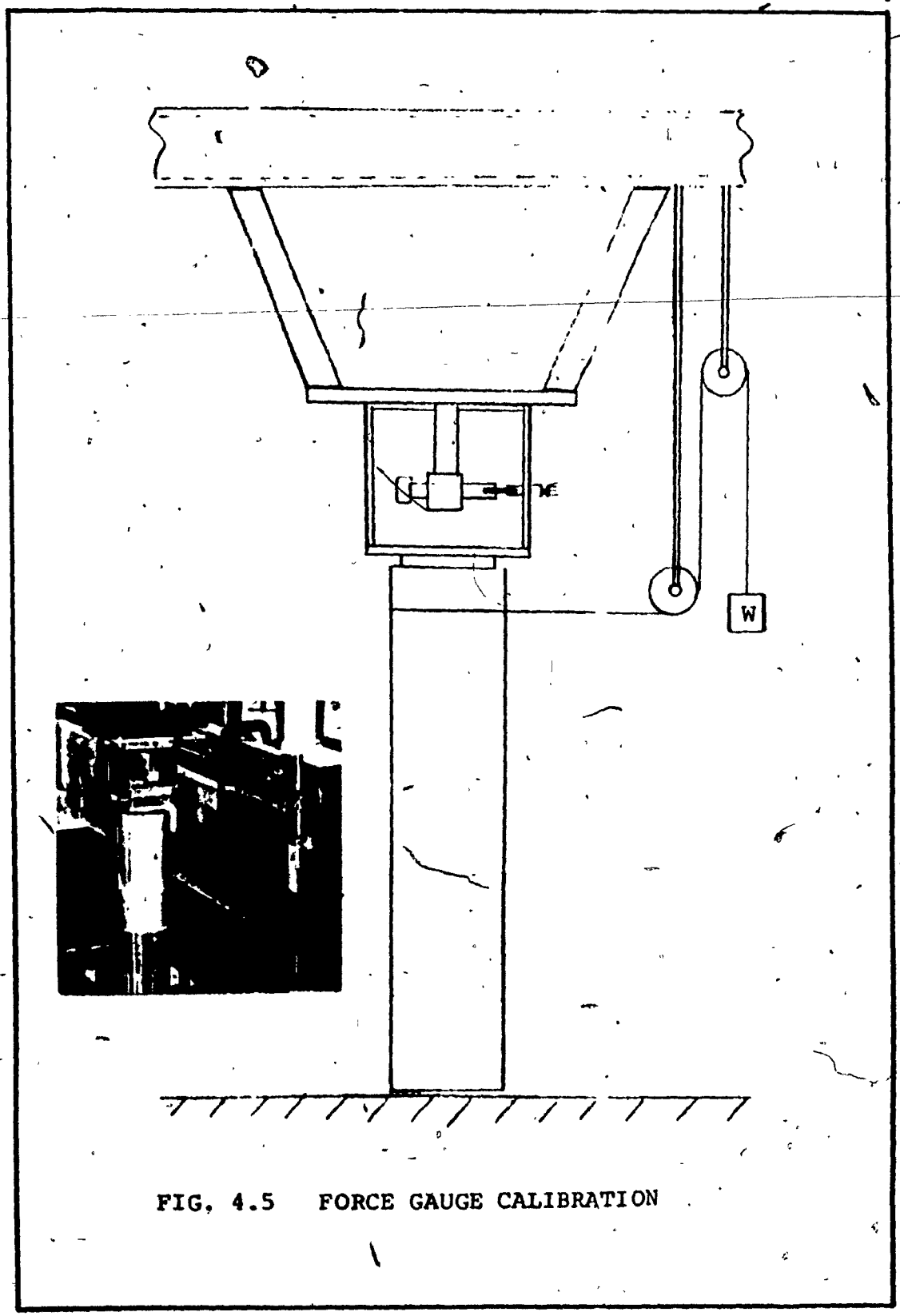

FIG, 4.5 FORCE GAUGE CALIBRATION

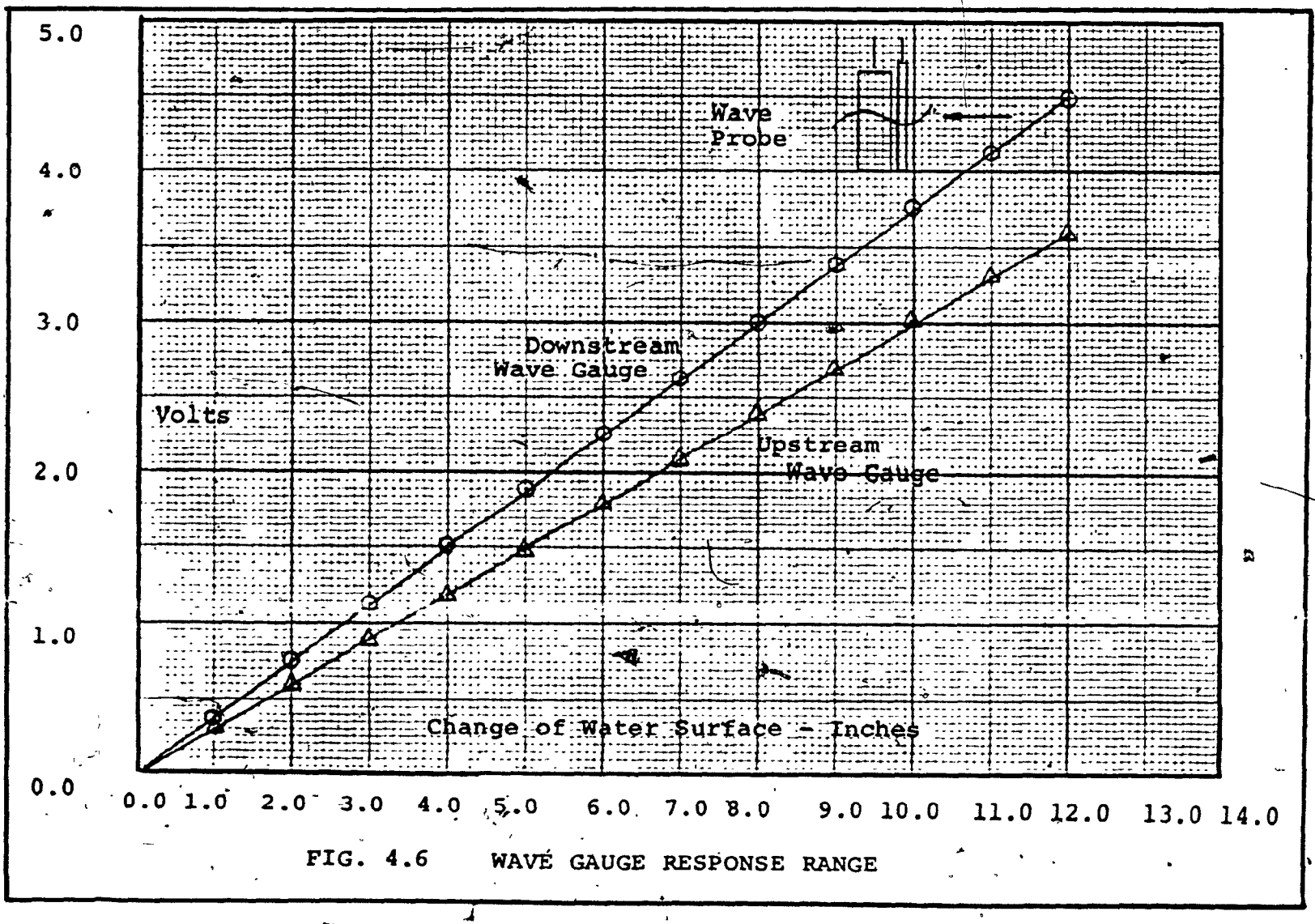

FIG. 4.6 WAVE GAUGE RESPONSE RANGE

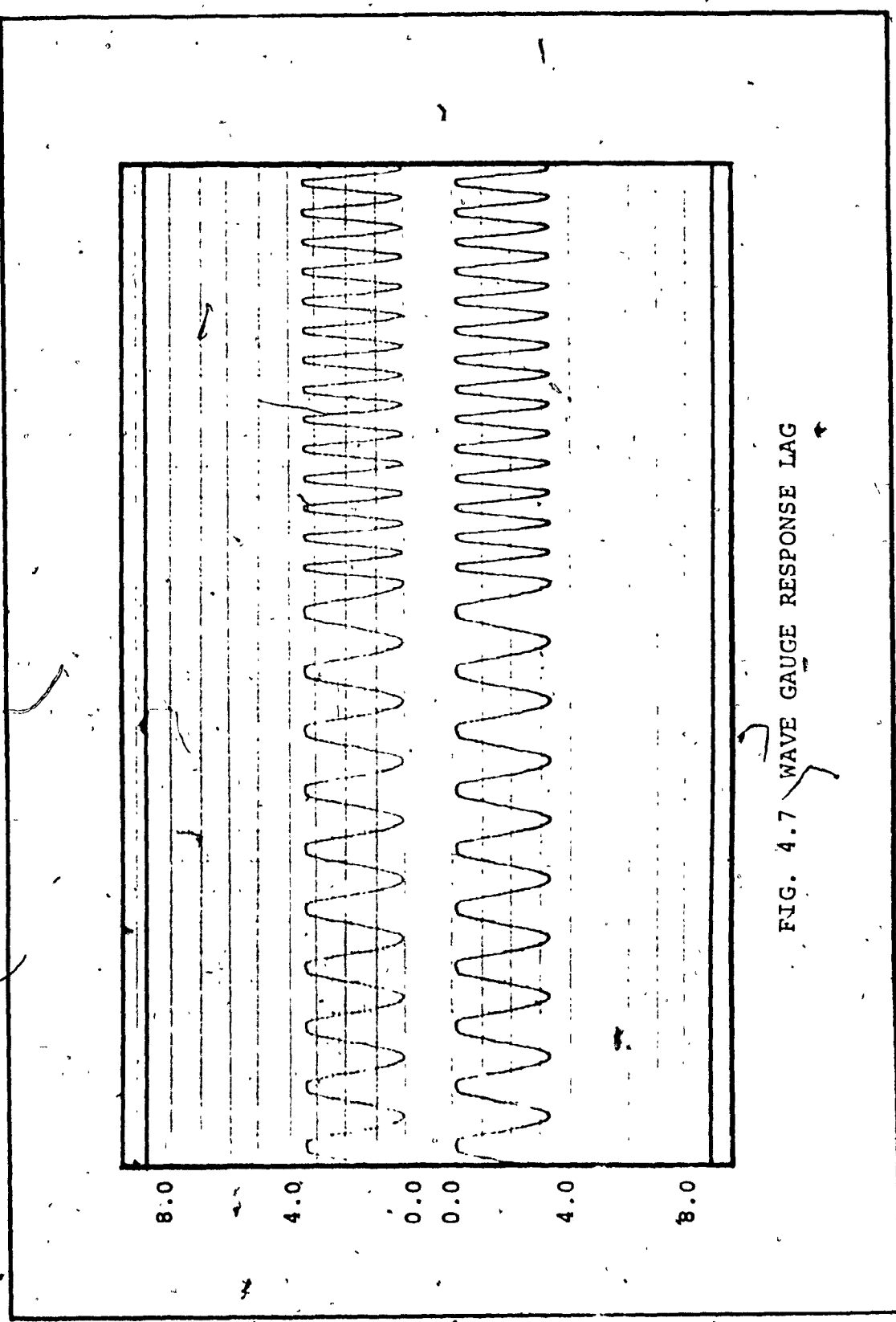

FIG. 4.7 WAVE GAUGE RESPONSE LAG

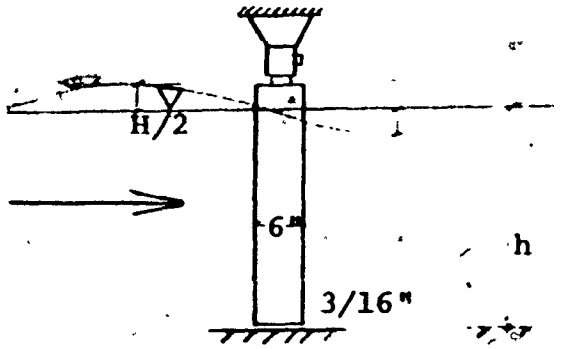

BASIC PARAMETERS

Water depth in the channel-h	2.50	<	h	>	3.79 feet
Wave amplitude - H -	0.17	<	H	>	0.83 feet
Wave length 'L'	7.0	<	L	>	38.5 feet
Time period of wave - L -	1.0	<	T	>	3.0 secs.
Angle of yaw - α^{o} -	6.5	<	α	>	14.0 degrees

DIMENSIONLESS PARAMETERS

Relative water depth h/L	0.481	<	h/L	>	0.097
Wave steepness - H/L	H/L	<	0.045	>	
Reynold's Number R	10^{4}	<	R	>	10^{5}
Keulegan Carpenter Number K.C.	1.0	<	K.C.	>	11.0
Drag coefficient, zero yaw	4.0	>	C_D	>	1.0
Drag coefficient, non-zero yaw	2.9	>	C_D	>	0.19
Lift coefficient (vertical pile) C_L	0.77	>	C_L	>	0.04

Table 5.1 RANGE OF VARIABLES

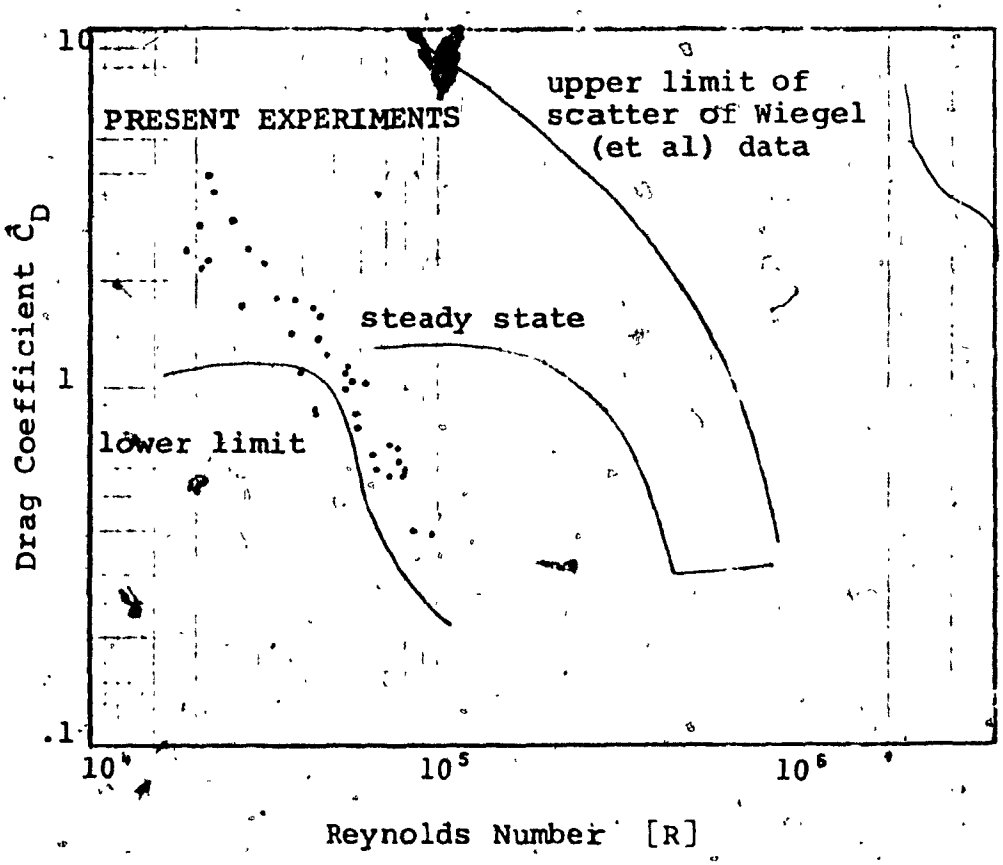

FIG. 5.2 RELATIONSHIP BETWEEN DRAG COEFFICIENTS AND REYNOLD'S NUMBERS FOR OSCILLATORY AND ACCELERATED FLOWS - ADAPTED FROM [13]

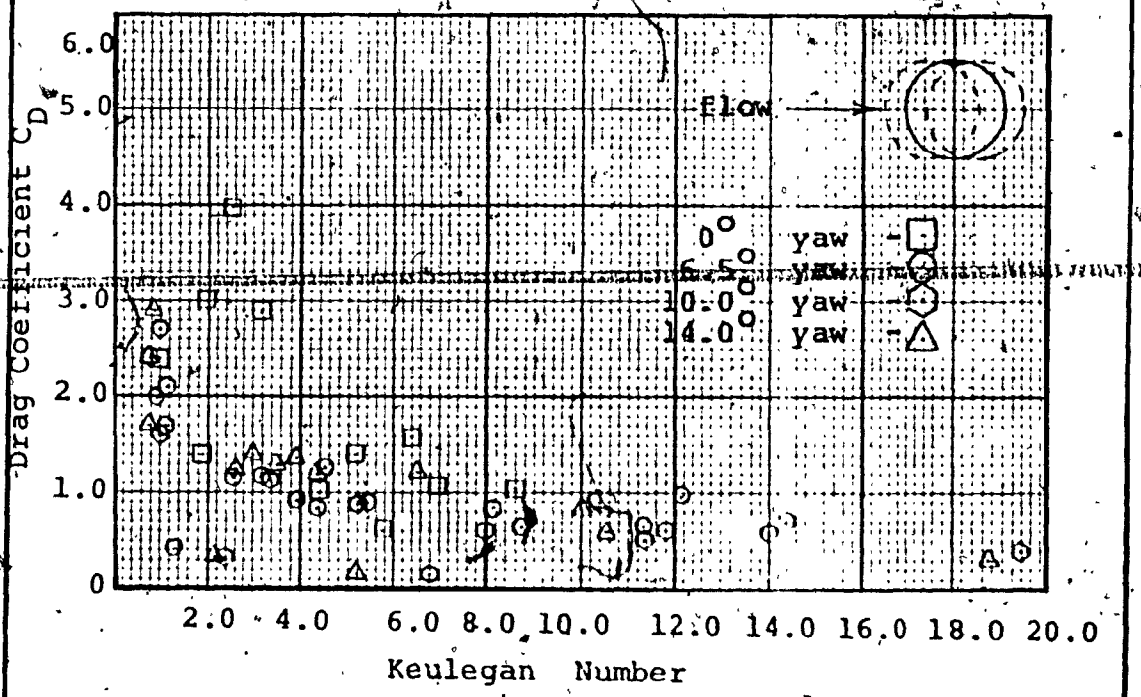

FIG.5.3 RELATIONSHIPS BETWEEN DRAG COEFFICIENT AND KEULEGAN NUMBER FOR VARYING DEGREES OF YAW. WATER DEPTH 3.79'

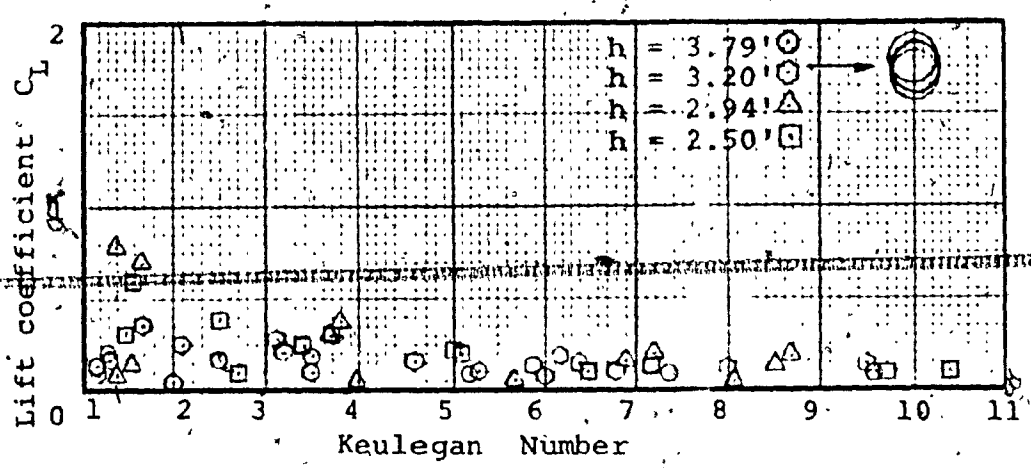

FIG. 5.4 RELATIONSHIP BETWEEN LIFT-COEFFICIENT AND KEULIGAN-CARPENTER NUMBER-VERTICAL PILE

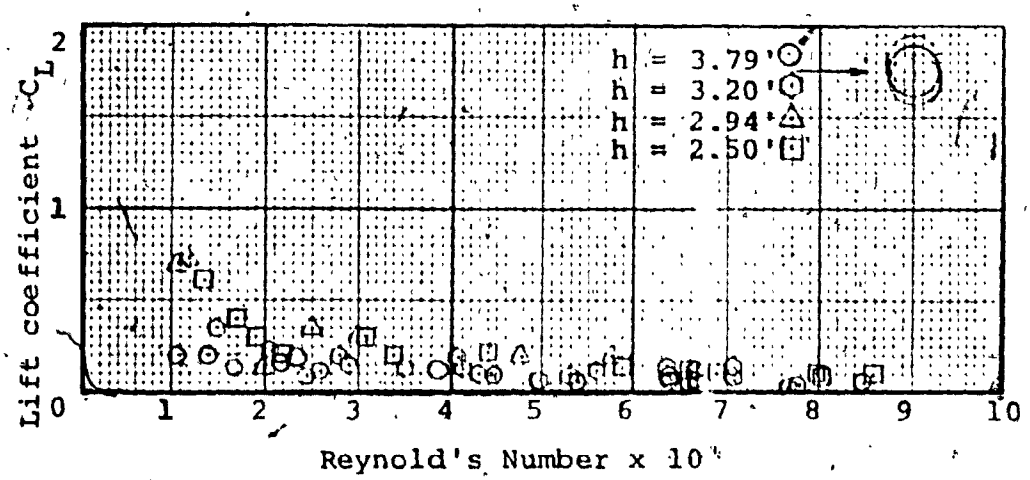

FIG. 5.5 RELATIONSHIP BETWEEN LIFT-COEFFICIENT AND REYNOLDS NUMBER-VERTICAL PILE

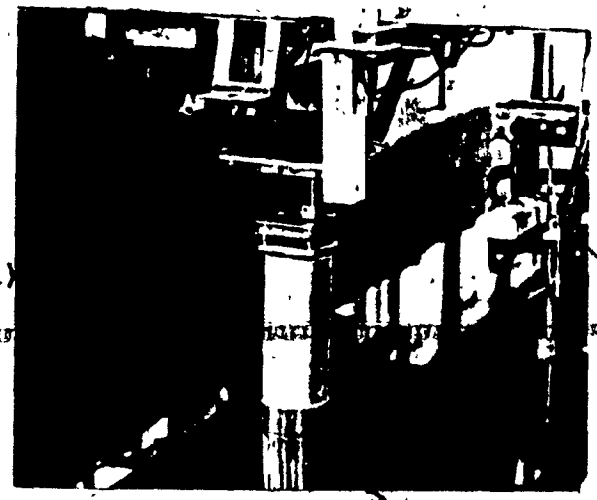

(1) Still Water Condition

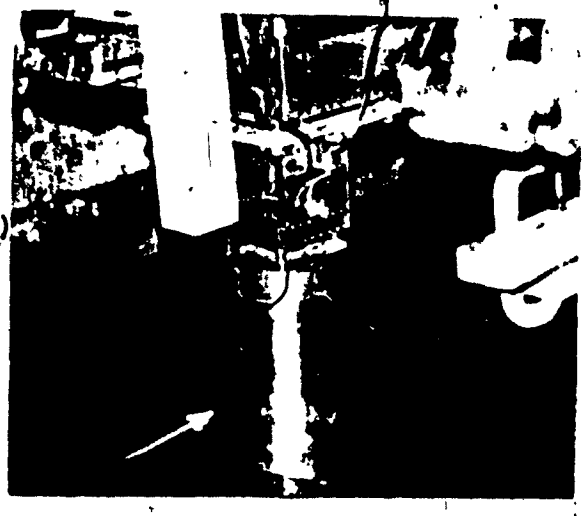

(2) Keulegan-Carpenter No. 1-2
No Separation-Amplitude of Motion Less Than Pile Diameter

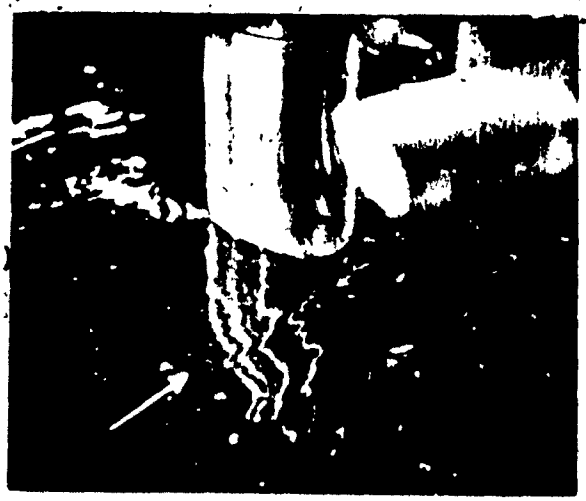

(3) Keulegan-Carpenter No. 2-3
Some Separation - At Least One Eddy is Shed

FIG. 5.6(a) PHOTOGRAPHIC OBSERVATIONS OF EDDY SHEDDING

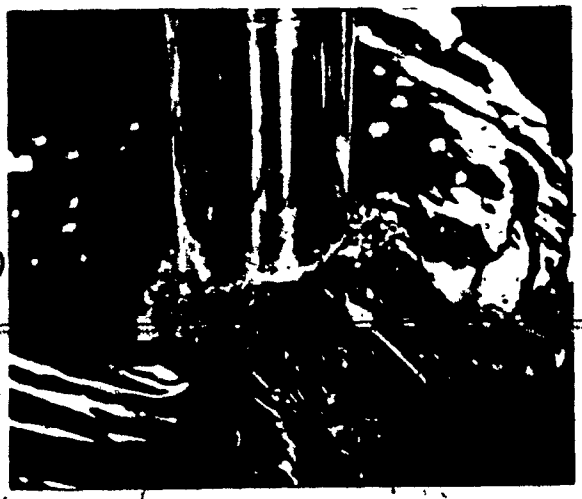

(4) Keulegan-Carpenter No. 3-4
More Than Two Eddies Are
Shed Within Half-Cycle-
VON KARMAN STREET

(5) Keulegan-Carpenter No. 4-6
Wake Becoming Turbulent.
Additional Eddies Are Shed
When Swept Back.

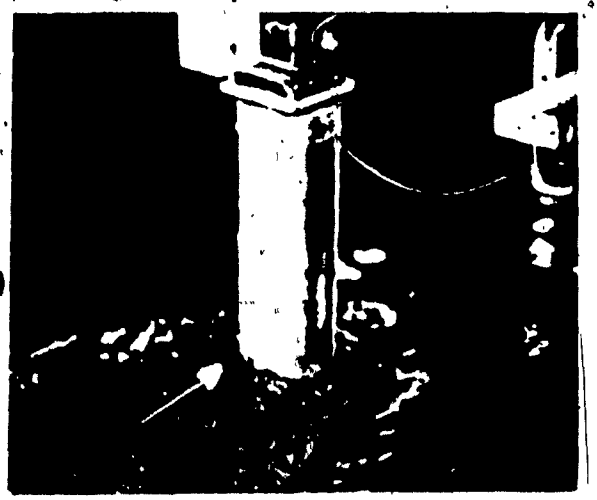

(6) Keulegan-Carpenter No. > 6
EXTREMELY TURBULENT

FIG. 5.6(b) PHOTOGRAPHIC OBSERVATIONS OF EDDY SHEDDING

APPENDIX B

TABLES

TABLE 1

SUMMARY OF COEFFICIENTS [17]

TABLE 1

SUMMARY OF COEFFICIENTS [17]

Source	D (ft)	d (ft)	Maximum Reynold Numbers from	Maximum Reynold Numbers to	Average C_d	Average C_m
Morrison [22], Laboratory (1954)	0.083	2	2×10^3	3×10^5	1.6	1.5
Wiegel [29] Ocean (1957)	0.5,1,2	50	3×10^4	9×10^5	0.6	2.5
Jen [14], Laboratory (1968)	0.5	3	5×10^3	2×10^4	...	2.04
			Irregular waves No. 1		...	2.20
			Irregular waves No. 2		...	2.08
Evans et al. [1,10,27,31] Ocean (1969)	2,3,4	33	10^4	6×10^7	0.585	1.5
	3	100	10^4	6×10^7	0.88	1.76
Steady flow	...	...	2×10^2	3×10^5	1.2	0
Hydrodynamic theory	...	...	...	...	0	2.0
Diffraction theory	...	...	...	...	0	2.0

TABLES 2(a),(b),(c),(d)

SUMMARY OF PRELIMINARY TESTS,

- DRAG FORCES

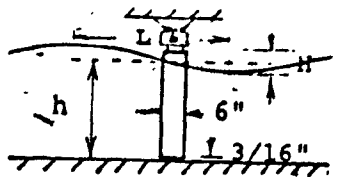
L
H
h
6"
3/16"

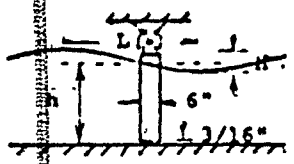
6"
1 3/16"

TABLE 2(a)

SUMMARY OF PRELIMINARY TESTS

Depth 'h' = 3.79 feet										0° YAW-DRAG
EXPERIMENTAL OBSERVATIONS						PRELIMINARY RESULTS				
Run No.	Chart Record No.	Time Period Sec.	Amplitude ft	Drag Force Oz.	Wave Length ft	Theory Wave Length	Drag Coefficient C_D	Reynolds No.	Particle Velocity ft/sec.	Keulegan No.
1	2131072	3.75	.27	14.80	38.50	39.05	2.85	210419	.421	3.17
2	3131072	3.75	.54	33.00	38.50	39.05	1.55	426049	.852	7.39
3	4131072	3.75	.72	39.40	38.50	39.05	1.02	572847	1.146	8.59
4	6131072	2.86	.27	23.00	28.50	28.53	3.98	221881	.444	2.54
5	7131072	2.86	.54	33.00	28.50	28.53	1.37	453176	.906	5.18
6	8131072	2.86	.72	46.00	28.50	28.53	1.04	612898	1.226	7.00
7	10111072	1.95	.27	23.20	17.00	17.08	2.97	257784	.516	2.01
8	11111072	1.95	.54	33.00	17.00	17.08	.97	539129	1.078	4.19
9	12111072	1.95	.72	29.50	17.00	17.08	.61	740761	1.482	5.76
10	13111072	1.25	.14	9.90	7.80	7.88	2.41	186889	.374	.93
11	14111072	1.25	.27	23.00	7.80	7.88	1.36	379522	.759	1.90

TABLE 2(b)

SUMMARY OF PRELIMINARY TESTS

Depth 'h' = 3.76 feet						6.5° YAW-DRAG				
EXPERIMENTAL OBSERVATIONS						PRELIMINARY RESULTS				
Run No.	Chart Record No.	Time Period Sec.	Amplitude ft	Drag Force Oz.	Wave Length ft	Theory Wave Length	Drag Coefficient C_D	Reynolds No.	Particle Velocity ft/sec.	Keulegan No.
201	1190573	3.75	.20	5.87	38.50	39.05	1.592	6317.1	.126	.95
202	2190573	3.75	.32	11.10	38.50	39.05	1.157	16440.0	.329	2.47
203	3190573	3.75	.43	22.20	38.50	39.05	1.262	30138.6	.603	4.52
204	4190573	3.75	.69	44.30	38.50	39.05	.944	80461.3	1.609	12.07
205	5190573	3.00	.21	12.70	28.50	29.96	2.628	8281.3	.166	.99
206	6190573	3.00	.43	17.50	28.50	29.96	.827	36243.3	.725	4.35
207	7190573	3.00	.60	27.00	28.50	29.96	.634	72958.3	1.459	8.76
208	8190573	3.00	.75	38.00	28.50	29.96	.555	117415.0	2.348	14.09
209	9190573	2.00	.19	12.70	17.54	17.74	1.975	11020.0	.220	.88
210	10190573	2.00	.35	26.00	17.54	17.74	1.126	39560.0	.791	3.17
211	11190573	2.00	.45	35.00	17.54	17.74	.885	67737.0	1.355	5.42
212	12190573	2.00	.63	52.00	17.54	17.74	.630	141150.0	2.829	11.32
213	13190573	1.00	.20	9.50	8.20	6.46	.339	48029.0	.961	1.92

TABLE 2(c)

SUMMARY OF PRELIMINARY TESTS

Depth 'h' = 3.79 feet						10° YAW-DRAG				
EXPERIMENTAL OBSERVATIONS						PRELIMINARY RESULTS				
Run No.	Chart Record No.	Time Period Sec.	Amplitude ft	Drag Force Qz.	Wave Length ft	Theory Wave Length ft	Drag Coefficient C_D	Reynolds No.	Particle Velocity	Keulegan No.
214	1180573	3.75	.22	9.40	38.50	39.05	2.120	7654.7	.153	1.15
215	2180573	3.75	.40	12.40	38.50	39.05	.825	25972.0	.519	3.90
216	3180573	3.75	.57	25.00	38.50	39.05	.801	53906.7	1.080	8.10
217	4180573	3.75	.75	37.60	38.50	39.05	.678	95865.4	1.917	14.38
218	5180573	3.00	.19	9.40	28.50	29.96	2.407	6752.7	.135	.81
219	6180573	3.00	.47	22.00	28.50	29.96	.872	43640.3	.873	5.24
220	7180573	3.00	.69	33.00	28.50	29.96	.581	98231.8	1.964	11.79
221	8180573	3.00	.87	34.50	28.50	29.96	.369	161787.6	3.236	19.42
222	9180573	2.00	.21	14.00	17.54	17.74	1.785	13557.8	.271	1.09
223	10180573	2.00	.36	28.00	17.54	17.74	1.153	42000.9	.840	3.36
224	11180573	2.00	.54	33.00	17.54	17.74	.567	100681.4	2.014	8.06
225	12180573	2.00	.63	42.00	17.54	17.74	.513	141450.8	2.829	11.32
226	13180573	1.00	.22	9.40	8.20	6.46	.274	59257.6	1.185	2.37

TABLE 2 (d)

SUMMARY OF PRELIMINARY TESTS

Depth 'h' = 3.79 feet						14° YAW DRAG				
EXPERIMENTAL OBSERVATIONS						PRELIMINARY RESULTS				
Run No.	Chart Record No.	Time Period Sec.	Amplitude ft	Drag Force Oz.	Wave Length ft	Theory Wave Length ft	Drag Coefficient C_D	Reynolds No.	Particle Velocity	Keulegan No.
227	1180573	3.75	.19	9.40	38.50	39.05	2.897	56972.5	.114	.85
228	2180573	3.75	.38	17.50	38.50	39.05	1.314	23375.3	.468	3.51
229	3180573	3.75	.42	19.50	38.50	39.05	1.192	28711.4	.574	4.31
230	4180573	3.75	.85	21.00	38.50	39.05	.295	124877.1	2.498	18.73
231	5180573	3.00	.19	9.30	28.50	29.96	2.417	8752.7	.135	.81
232	6180573	3.00	.36	20.00	28.50	29.96	1.401	25058.4	.501	3.01
233	7180573	3.00	.41	26.60	28.50	29.96	1.422	32821.6	.656	3.94
234	8180573	3.00	.64	39.00	28.50	29.96	.818	83665.9	1.673	10.04
235	9180573	2.00	.18	9.40	17.54	17.74	1.674	9856.4	.197	.79
236	10180573	2.00	.32	23.00	17.54	17.74	1.233	32722.4	.654	2.62
237	11180573	2.00	.49	26.00	17.54	17.74	.560	81453.7	1.629	6.52
238	12130573	2.00	.61	43.00	17.54	17.74	.573	131681.6	2.634	10.54
239	13180573	1.00	.21	8.00	8.20	6.46	.263	53470.3	1.069	2.14
240	14180573	1.00	.31	11.00	8.20	6.46	.150	128425.3	2.568	5.14

TABLES 3(a), (b), (c), (d)

SUMMARY OF PRELIMINARY TESTS

– LIFT FORCES

TABLE 3(a)

SUMMARY OF PRELIMINARY TESTS

Depth 'h' = 3.79 feet						LIFT FORCE						
EXPERIMENTAL OBSERVATIONS						PRELIMINARY RESULTS						
Run No.	Chart Record No.	Time Period Sec.	Amplitude 'h' ft	Lift Force Oz.	Wave Length 'L' ft	Theory Wave Length ft	Lift Coefficient C_L	H/L	h/L	Reynolds No.	Particle Velocity ft/sec.	Keulegan No.
101	1131072	3.75	.18	.55	38.50	39.05	.240	.005	.097	13971.5	.279	2.10
102	2131072	3.75	.30	1.16	38.50	39.05	.181	.008	.097	23411.5	.468	3.51
103	3131072	3.75	.50	2.20	38.50	39.05	.121	.013	.097	39376.4	.788	5.90
104	4131072	3.75	.80	4.24	38.50	39.05	.088	.020	.097	63890.1	1.278	9.58
105	5061072	2.86	.14	.31	28.50	28.53	.203	.005	.133	11391.1	.228	1.30
106	6061072	2.86	.27	.92	28.50	28.53	.159	.009	.133	22188.1	.444	2.54
107	7061072	2.86	.54	1.76	28.50	28.53	.073	.019	.133	45317.6	.906	5.18
108	8061072	2.86	.75	3.53	28.50	28.53	.073	.026	.133	63096.4	1.280	7.31
109	9061072	1.95	.18	.46	17.00	17.08	.137	.011	.222	16933.4	.339	1.32
110	10061072	1.95	.27	.85	17.00	17.08	.109	.016	.222	25778.5	.516	2.01
111	11061072	1.95	.54	1.69	17.00	17.08	.050	.032	.222	53912.9	1.078	4.19
112	12061072	1.95	.75	2.46	17.00	17.08	.035	.044	.222	77551.4	1.551	6.03
113	13061072	1.25	.18	.53	7.80	7.88	.076	.023	.481	24413.3	.488	1.22

TABLE 3(b)

SUMMARY OF PRELIMINARY TESTS

Depth 'h' = 3.34 feet						LIFT FORCE						
EXPERIMENTAL OBSERVATIONS						PRELIMINARY RESULTS						
Run No:	Chart Record No.	Time Period Sec.	Amplitude 'h' ft	Lift Force Oz.	Wave Length 'L' ft	Theory Wave Length ft	Lift Coefficient C_L	H/L	h/L	Reynolds No.	Particle Velocity ft/sec.	Keulegan No.
114	1131072	3.75	.25	1.00	38.50	37.11	.226	.007	.090	20679.0	.414	3.10
115	2131072	3.75	.49	2.34	38.50	37.11	.135	.013	.090	40973.7	.819	6.15
116	3131072	3.75	.63	3.10	38.50	37.11	.107	.017	.090	53022.6	1.060	7.95
117	4131072	3.75	.75	5.60	38.50	37.11	.134	.020	.090	63478.4	1.270	9.52
118	5141072	2.86	.17	.78	28.00	27.26	.352	.006	.123	14635.0	.293	1.67
119	6141072	2.86	.32	1.56	28.00	27.26	.194	.012	.123	28975.0	.557	3.19
120	7141072	2.86	.46	2.65	28.00	27.26	.156	.017	.123	40494.3	.810	4.63
121	8141072	2.86	.63	3.90	28.00	27.26	.119	.023	.123	56205.7	1.124	6.42
122	10141072	2.00	.43	1.85	17.00	17.14	.097	.025	.195	42953.8	.859	3.44
123	11141072	2.00	.64	2.50	17.00	17.14	.065	.037	.195	66101.8	1.322	5.29
124	12141072	2.00	.80	3.74	17.00	17.14	.050	.047	.195	84776.5	1.696	6.78
125	13141072	1.00	.17	1.25	7.00	5.97	.141	.028	.559	29253.4	.585	1.17
126	14141072	1.00	.40	1.73	7.00	5.97	.028	.067	.559	77673.7	1.553	3.11

TABLE 3(c)

SUMMARY OF PRELIMINARY TESTS

Depth 'h' = 2 84 feet						LIFT FORCE						
EXPERIMENTAL OBSERVATIONS						PRELIMINARY RESULTS						
Run No.	Chart Record No.	Time Period Sec.	Amplitude 'h' ft	Lift Force Oz.	Wave Length 'L' ft	Theory Wave Length ft	Lift Coefficient C_L	H/L	h/L	Reynolds No.	Particle Velocity ft/sec.	Keulegan No.
127	1271072	3.75	.13	.81	34.80	34.98	.697	.004	.084	1.1295.4	.226	1.69
128	2271072	3.75	.29	2.02	34.80	34.98	.344	.008	.084	2.5379.4	.508	3.81
129	3271072	3.75	.54	4.01	34.80	34.98	.193	.015	.015	4.7806.9	.956	7.17
130	4271072	3.75	.65	5.70	34.80	34.98	.187	.019	.019	5.7845.3	1.157	8.68
131	5271072	3.00	.13	.95	27.00	27.20	.772	.005	.005	1.1619.4	.232	1.39
132	6271072	3.00	.34	2.58	27.00	27.20	.298	.013	.013	3.0841.3	.617	3.70
133	7271072	3.00	.62	4.05	27.00	27.20	.135	.023	.023	5.7390.8	1.148	6.89
134	8271072	3.00	.76	6.00	27.00	27.20	.130	.028	.028	7.1082.8	1,422	8.53
135	9271072	2.00	.20	.50	16.00	16.39	.137	.012	.012	2.0007.6	.400	1.60
136	10271072	2.00	.48	1.28	16.00	16.39	.056	.029	.029	5.0210.3	1.004	4.01
137	11271072	2.00	.66	1.80	16.00	16.39	.039	.040	.040	7.1081.4	1.422	5.69
138	12271072	2.00	.90	3.60	16.00	16.39	.039	.055	.055	10.0822.5	2.016	8.07
139	13271072	1.00	.20	.90	5.00	5.06	.078	.040	.040	3.5620.3	.712	1.43
140	14271072	1.00	.48	2.02	5.00	5.06	.021	.095	.095	10.1719.2	2.034	4.07

TABLE 3(d)

SUMMARY OF PRELIMINARY TESTS

Depth 'h' = 2.50 feet						LIFT FORCE							
EXPERIMENTAL OBSERVATIONS						PRELIMINARY RESULTS							
Run No.	Chart Record No.	Time Period Sec.	Amplitude 'h' ft	Lift Force Oz.	Wave Length 'L' ft	Theory Wave Length ft	Lift Coefficient C_L	H/L	h/L	Reynolds No.	Particle Velocity ft/sec.	Keulegan No.	
141	1291072	3.75	.18	.88	32.00	32.38	.399	.006	.077	1.6875.8	.338	2.53	
142	2291072	3.75	.36	1.76	32.00	32.38	.196	.011	.077	3.4030.5	.681	5.10	
143	3291074	3.75	.72	3.56	32.00	32.38	.096	.022	.077	6.8238.9	1.385	10.37	
144	4291072	3.75	.83	5.00	32.00	32.38	.100	.026	.077	8.0251.4	1.605	12.04	
145	5291072	3.00	.14	.85	25.00	25.33	.608	.006	.099	1.3428.1	.269	1.61	
146	6291072	3.00	.32	2.40	25.00	25.33	.321	.013	.099	3.1086.4	.622	3.73	
147	7291072	3.00	.60	3.56	25.00	25.33	.130	.024	.099	5.9493.2	1.190	7.14	
148	8291072	3.00	.80	5.50	25.00	25.33	.109	.032	.099	8.0531.5	1.611	9.66	
149	9291072	1.88	.18	.90	14.00	14.31	.308	.013	.175	1.9417.5	.388	1.46	
150	10181172	1.88	.40	3.50	14.00	14.31	.224	.028	.175	4.4897.5	.898	3.38	
151	11181172	1.88	.57	4.26	14.00	14.31	.126	.040	.175	6.6004.2	1.320	4.96	
152	12181172	1.88	.72	5.50	14.00	14.31	.097	.050	.175	8.5727.3	1.715	6.45	
153	3181172	1.00	.13	.72	5.00	5.05	.188	.026	.495	2.2225.0	.445	.89	
154	4181172	1.00	.34	1.60	5.00	5.05	.047	.067	.495	6.6214.1	1.324	2.65	

APPENDIX C

COMPUTER PROGRAM LISTINGS

Program listing zero yaw - Drag Force
Program listing - Lift Force
Program listing - non zero yaw - Drag Force

```
      PROGRAM GHULAM(INPUT,OUTPUT,TAPE5=INPUT)
      DIMENSION TA(16),AAA(16)
      DIMENSION RNO(16)
      DIMENSION CON(16),CO(16)
      DIMENSION ELL(16),FLL(16)
      DIMENSION T(16),H(16),FL(16)
      DIMENSION C(16),DLL(16),REY(16),CAR(16),STR(16),AA(16),BB(16),CC(16)
      DIMENSION Z(16),Y(16),TT(16),V(16)
      DIMENSION F(16),EL(16)
      DIMENSION DITTO(16)
C     D IS DEPTH OF WATER IN THE CHANNEL IN FT.
      D=2.50
C     T IS THE TIME PERIOD OF WAVE IN SECOND
      READ(5,12)(T(N),N=1,16)
12    FORMAT(8F10.5)
C     H IS THE WAVE HIGHT IN FT
      READ(5,13)(H(N),N=1,16)
13    FORMAT(8F10.5)
C     DB IS THE TEST BODY DIAMETER
      DB=0.50000
      G=32.1740
      PI=3.1420
C     ELL IS THE EXPERIMENTAL WAVE LENGTH FROM DATA
      READ(5,14)(ELL(N),N=1,16)
14    FORMAT(8F10.5)
      READ(5,15)(F(N),N=1,16)
15    FORMAT(8F10.5)
      READ(5,16)(RNO(N),N=1,15)
16    FORMAT(1015)
      PRINT 3,D
3     FORMAT(14H  LIFT, DEPTH=,F6.3)
      PRINT 4
4     FORMAT(1H0,2X,3HRUN,1X,2HNO,2X,10HTIMEPERIOD,2X,9HAMPLITUDE,1X,9HL
     6IFTFORCE,1X,4HDASA,1X,10HWAVELENGTH,1X,10HATPYTHEORY,1X,2HWL,1X,4H
     5LIFT,1X,5HCOEFF,1X,3HH/L,4X,3HD/L,1X,7HREYNOLD,1X,2HNO,3X,6HPARTCL
     4,1X,3HVEL,1X,8HKEULEGAN,1X,2HNO)
      PRINT 5
5     FORMAT(1H0,12X,7HSECONDS,6X,4HFEET,5X,8HPOUND/16,7X,4HFEET,6X,4HF
     6EET,4X,9HFEET/SECS)
      DO 100 N=1,16
      N=N
C     C IS THE THEORITICAL WAVE CELERITY IN FPS
      AAA(N)=(2*PI*D/ELL(N))
      TA(N)=(2.7183**AAA(N)-1/2.7183**AAA(N))/(2.7183**AAA(N)+1/2.7183**
     6AAA(N))
      CON(N)=(G*ELL(N))/(2*PI)
      C(N)=(CON(N)*TA(N))**0.5
      CO(N)=(G*(T(N)**2))/(2*PI)
      DLL(N)=CO(N)*TA(N)
C     EL IS THE ACTUAL VALUE OF WAVE LENGTH FROM EXPERIMENTAL DATA
      EL(N)=C(N)*T(N)
C     U IS THE PARTICAL VELOCITY MAX. IN FPS
      Z(N)=((2*PI*(D+(H(N)/2)))/EL(N))
      Y(N)=((2.7183**Z(N)+(1/2.7183**Z(N)))/2)
      TT(N)=2*PI*D/EL(N)
      V(N)=((2.7183**TT(N)-1/2.7183**TT(N))/2)
      U(N)=(PI*H(N)/T(N)*(Y(N)/V(N)))
      VNU=0.00001
      AREA=DB*D
      RHO=1.937
      DITTO(N)=RHO*AREA*U(N)*U(N)
      CL(N)=F(N)/DITTO(N)
      REY(N)=(U(N)*DB)/VNU
C     CAR(N) IS THE CARPENTER KEULEGAN NUMBER
      CAR(N)=(U(N)*T(N))/DB
C     STR(N) IS THE STRAHAUL NUMBER
      STR(N)=(DB)/(T(N)*U(N))
      AA(N)=H(N)/EL(N)
      BB(N)=D/EL(N)
      PRINT2,(RNO(N),T(N),H(N),F(N),ELL(N),EL(N),CL(N),AA(N),BB(N),REY(N
     6),U(N),CAR(N))
2     FORMAT(1H0,1X,I9,(11(F10.3,1X)))
100   CONTINUE
      PRINT 6
6     FORMAT(1H0,4HNOTE,4X,4HLAST,1X,9HTWO/THREE,1X,4HRUNS,1X,2HTO,1X,2H
     6BE,1X,11HDISREGARDED,2X,5HDUMMY,1X,6HVALUES,1X,2HOF,1X,6HDATA,1X,6
     5HREADIN,1X,3HDUE,1X,2HTO,1X,7HTOOMUCH,1X,10HTURBULANCE,1X,6HDURING
     4,1X,11HEXPERIMENT.)
      STOP
      END.
```

```
      PROGRAM GROULAM(INPUT,OUTPUT,TAPE5=INPUT)
      DIMENSION YV(16),VU(16),VO(16),DITTO(16),AO(16),AVSM(16)
      DIMENSION CM(16)
      DIMENSION A(16),P(16),CRM(16),CU(16)
      DIMENSION TA(16),AAA(16)
      DIMENSION RNO(16)
      DIMENSION CON(16),CO(16)
      DIMENSION ELL(16),ELLL(16)
      DIMENSION T(16),H(16),EL(16)
      DIMENSION C(16),U(16),REY(16),CAR(16),STR(16),AA(16),BB(16),CC(16)
      DIMENSION Z(16),Y(16),TT(16),V(16)
      DIMENSION F(16),CL(16)
      DIMENSION DITTO(16)
C     D IS DEPTH OF WATER IN THE CHANNEL IN FT.
      D=3.29
C     T IS THE TIME PERIOD OF WAVE IN SECOND
      READ(8,12)(T(N),N=1,16)
12    FORMAT(8F10.5)
C     H IS THE WAVE HIGHT IN FT.
      READ(8,13)(H(N),N=1,16)
13    FORMAT(8F10.5)
C     DB IS THE TEST BODY DIAMETER
      DB=0.50000
      G=32.174
      PI=3.1420
C     ELL IS THE EXPERIMENTAL WAVE LENGTH FROM DATA
      READ(8,14)(ELL(N),N=1,16)
14    FORMAT(8F10.5)
      READ(8,15)(F(N),N=1,16)
15    FORMAT(8F10.5)
      READ(8,16)(RNO(N),N=1,16)
16    FORMAT(10I8)
      READ(8,17)(F(N),N=1,16)
17    FORMAT(8F10.5)
      PRINT 3,D
3     FORMAT(14H DRAG  DEPTH=,F4.3)
      PRINT 4
4     FORMAT(1H0,2X,3HRUN,1X,2HNO,2X,10HTIMEPERIOD,2X,9HAMPLITUDE,1X,9HO
     6MAGFORCE,1X,4HDATA,1X,10HAVELENGTH,1X,10HTHEORY,1X,2HHL,1X,4H
     5DRAG,1X,5HCUEFF,1X,3HCMC,6X,3HACL,1X,7HREYNOLD,1X,2HNO,1X,6HPARTCL
     4,1X,3HVEL,1X,8HEULEGAN,1X,2HNO)
      PRINT 5
5     FORMAT(1H0,12X,7HSECONDS,6X,4HFEET, 5X,8HPOUND/16,7X,4HFEET,6X,4HF
     6EET,47X,9HFEET/SECS)
      DO 100 N=1,16
      N=N
C     C IS THE THEORETICAL WAVE CELERITY IN FPS
      AAA(N)=(2*PI*D/ELL(N))
      TA(N)=(2.7183**AAA(N)-1/2.7183**AAA(N))/(2.7183**AAA(N)+1/2.7183**
     6AAA(N))
      CON(N)=(G*ELL(N))/(2*PI)
      C(N)=(CON(N)*TA(N))**0.5
      CO(N)=(G*(T(N)**2))/(2*PI)
      ELLL(N)=CO(N)*TA(N)
C     EL IS THE ACTUAL VALUE OF WAVE LENGTH FROM EXPERIMENTAL DATA.
      EL(N)=C(N)*T(N)
C     U IS THE PARTICAL VELOCITY MAX. IN FPS
      Z(N)=((2*PI*(D+(H(N)/2)))/EL(N))
      Y(N)=((2.7183**Z(N)+(1/2.7183**Z(N)))/2)
      TT(N)=2*PI*D/EL(N)
      V(N)=((2.7183**TT(N)-1/2.7183**TT(N))/2)
      U(N)=(PI*H(N)/T(N)*(Y(N)/V(N)))
      VOL=((PI*DB*DB*D)/4)
      VNU=0.00001
      AREA=DB*D
      RHO=1.937
      DITTO(N)=H*RHO*AREA*U(N)*U(N)
      CO(N)=F(N)/DITTO(N)
C     A IS THE ACCELERATION VALUE
      A(N)=((2*PI*PI*H(N))/(T(N)*T(N)))*(Y(N)/V(N))
      CRM(N)=1.0*RHO*VOL*A(N)
      CM(N)=F(N)/CRM(N)
      REY(N)=(U(N)*DB)/VNU
C       CAR(N) IS THE CARPENTER EULEGAN NUMBER
      CAR(N)=(U(N)*T(N))/DB
C     STR(N) IS THE STRAHAUL NUMBER
      STR(N)=(DB)/(T(N)*U(N))
      AA(N)=H(N)/EL(N)
      BB(N)=D/EL(N)
      PRINT2,(RNO(N),T(N),H(N),F(N),ELL(N),EL(N),CO(N),CM(N),A(N),REY(N)
     6,U(N),CAR(N))
2     FORMAT(1H0,1X,18,(11(F10.3,1X)))
100   CONTINUE
      PRINT 6
6     FORMAT(1H0,4HNOTE,4X,4HLAST,1X,9H1NO/THREE,1X,4HRUNS,1X,2HTO,1X,2H
     6BE,1X,11HDISREGARDED,2X,5HDUMMY,1X,6HVALUES,1X,2HOF,1X,4HDATA,1X,6
     5HREADI,N,1X,3HUSE,1X,2H10,1X,7HTOOMUCH,1X,10HTURBULANCE,1X,6HDURING
     4,1X,11HEXPERIMENT.)
      STOP
      END
```

```
      PROGRAM GMULAM(INPUT,OUTPUT,TAPE8=INPUT)
      DIMENSION CORN(16)
      DIMENSION VV(16),VU(16),VO(16),DUTTO(16),AO(16),AVSM(16)
      DIMENSION CM(16)
      DIMENSION A(16),FI(16),CKN(16),CU(16)
      DIMENSION TA(16),AAA(16)
      DIMENSION RNO(16)
      DIMENSION CON(16),CO(16)
      DIMENSION ELL(16),ELLL(16)
      DIMENSION T(16),H(16),EL(16)
      DIMENSION C(16),U(16),REY(16),CAR(16),STR(16),AA(16),BB(16),CC(16)
      DIMENSION Z(16),V(16),TT(16),V(16)
      DIMENSION F(16),EL(16)
      DIMENSION DITTO(16)
C     ALFA IS EQUAL TO 6.5 DEGREES
C     D IS DEPTH OF WATERIN THE CHANNEL IN FT.
      D=3.79
C     T IS THE TIME PERIOD OF WAVE IN SECOND
      READ(8,12)(T(N),N=1,16)
12    FORMAT(8F10.5)
C     H IS THE WAVE HIGHT IN FT
      READ(8,13)(H(N),N=1,16)
13    FORMAT(8F10.5)
C     DB IS THE TEST BODY DIAMETER
      DB=0.50000
      G=32.1740
      PI=3.1420
C     ELL IS THE EXPERIMENTAL WAVE LENGTH FROM DATA
      READ(8,14)(ELL(N),N=1,16)
14    FORMAT(8F10.5)
      READ(8,15)(F(N),N=1,16)
15    FORMAT(8F10.5)
      READ(8,16)(RNO(N),N=1,16)
16    FORMAT(10I8)
      READ(8,17)(FI(N),N=1,16)
17    FORMAT(8F10.5)
      PRINT 3,D
3     FORMAT(14H  DRAG  DEPTH=,F8.3)
      PRINT 4
4     FORMAT(1H0,2X,3HRUN,1X,2HNO,2X,10HTIMEPERIOD,2X,9HAMPLITUDE,1X,9HD
     6RAGFORCE,1X,4HDATA,1X,10HWAVELENGTH,1X,10HAIRYTHEORY,1X,2HWL,1X,4H
     5DRAG,1X,5HCOEFF,1X,3HCMC,6X,3HACL,1X,7HREYNOLD,1X,2HNO,1X,6HPARTCL
     4/1X,3HVEL,1X,8HREULEGAN,1X,2HNO)
      PRINT 5
5     FORMAT(1HU,12X,7HSECONDS,6X,4HFEET,5X,8HPOUND/16,7X,4HFEET,6X,4HF
     6EET,4X,9HFEET/SECS)
      DO 100 M=1,16
      N=M
C     C IS THE THEORETICAL WAVE CELERITY IN FPS
      AAA(N)=(2*PI*D/ELL(N))
      TA(N)=(2.7183**AAA(N)-1/2.7183)**AAA(N))/(2.7183**AAA(N)+1/2.7183**
     6AAA(N))
      CON(N)=(G*ELL(N))/(2*PI)
      C(N)=(CON(N)*TA(N))**0.5
      CO(N)=(G*(T(N)**2))/(2*PI)
      ELLL(N)=CO(N)*TA(N)
C     EL IS THE ACTUAL VALUE OF WAVE LENGTH FROM EXPERIMENTAL DATA
      EL(N)=C(N)*T(N)
C     U IS THE PARTICAL VELOCITY MAX. IN FPS
      Z(N)=((2*AI*(D-(H(N)/2)))/EL(N))
      Y(N)=((2.7183**Z(N)+(1/2.7183**Z(N)))/2)
      YY(N)=((2.7183**Z(N)-(1/2.7183**Z(N)))/2)
      TT(N)=2*PI*D/EL(N)
      V(N)=((2.7183**TT(N)-1/2.7183**TT(N))/2)
      U(N)=(PI*H(N)/T(N))*(Y(N)/V(N))
      VU(N)=(PI*H(N)/T(N))*(YV(N)/V(N))
      VO(N)=(U(N)**2+VU(N)**2)
      VOL=((PI*DB*DB*D)/4)
      DOL=D*0.9966
      VNU=0.00001
      AOL=DOL*DB
      RHO=1.937
      VOLO=((PI*DB*DB*D)/4)
      DOTTO(N)=B*RHO*AOL*VO(N)
      CO(N)=F(N)/DOTTO(N)
C     A IS THE ACCELERATION VALUE
      A(N)=((2*PI*PI*H(N))/(T(N)*T(N)))*(Y(N)/V(N))
      AO(N)=((2*PI*PI*H(N))/(T(N)*T(N)))*(YV(N)/V(N))
      AVSM(N)=(A(N)**2+AO(N)**2)**0.5
      CORN(N)=16*RHO*VOLU*AVSM(N)
      CM(N)=F(N)/CORN(N)
      REY(N)=(VO(N)*DB)/VNU
C     CAR(N) IS THE CARPENTER REULEGAN NUMBER
      CAR(N)=(VO(N)*T(N))/DB
C     STR(N) IS THE STRAHAUL NUMBER
      STR(N)=(DB/(T(N)*U(N)))
      AA(N)=H(N)/EL(N)
      BB(N)=D/EL(N)
      PRINT2,(RNO(N),T(N),H(N),F(N),ELL(N),EL(N),CO(N),CM(N),AVSM(N),REY
     6(N),VO(N),CAR(N))
2     FORMAT(1H0,1X,I8,(11(F10.3,1X)))
100   CONTINUE
      PRINT 6
6     FORMAT(1H0,4HNUTE,4X,4HLAST,1X,9HTWO/THREY,1X,4HRUNS,1X,2HTO,1X,2H
     6AE,1X,11HUSREULEAHOLD,2X,5HUUMMY,1X,4HVALUES,1X,2HOF,1X,4HDATA,1X,6
     5HREADIN,1X,3HOVE,1X,2HTO,1X,7HTODMUCH,1X,10HTUNBULANCE,1X,6HDURING
     6,1X,11HEXPERIMENT.)
      STOP
      END
```